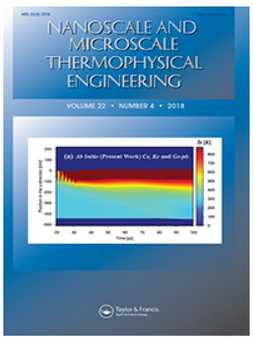

Nanoscale and Microscale Thermophysical Engineering

ISSN: 1556-7265 (Print) 1556-7273 (Online) Journal homepage: https://www.tandfonline.com/loi/umte20

Pool boiling heat transfer of water and nanofluid outside the surface with higher roughness and different wettability

Wen-Tao Ji, Peng-Fei Zhao, Chuang-Yao Zhao, Jing Ding & Wen-Quan Tao

To cite this article: Wen-Tao Ji, Peng-Fei Zhao, Chuang-Yao Zhao, Jing Ding & Wen-Quan Tao (2018) Pool boiling heat transfer of water and nanofluid outside the surface with higher roughness and different wettability, Nanoscale and Microscale Thermophysical Engineering, 22:4, 296-323, DOI: 10.1080/15567265.2018.1497110

To link to this article: https://doi.org/10.1080/15567265.2018.1497110

Published online: 07 Sep 2018.

NANOSCALE AND MICROSCALE THERMOPHYSICAL ENGINEERING
2018, VOL. 22, NO. 4, 296–323
https://doi.org/10.1080/15567265.2018.1497110

Taylor & Francis
Taylor & Francis Group

ARTICLE

Pool boiling heat transfer of water and nanofluid outside the surface with higher roughness and different wettability

Wen-Tao Ji, Peng-Fei Zhao, Chuang-Yao Zhao, Jing Ding, and Wen-Quan Tao

Key Laboratory of Thermo-Fluid Science and Engineering of MOE, Xi'an Jiaotong University, Xi'an, China

ABSTRACT

In order to investigate the effect of surface wettability on the pool boiling heat transfer, nucleate pool boiling experiments were conducted with deionized water and silica based nanofluid. A higher surface roughness value in the range of 3.9 ~ 6.0μm was tested. The contact angle was from 4.7° to 153°, and heat flux was from 30kW/m^2 to 300kW/m^2. Experimental results showed that hydrophilicity diminish the boiling heat transfer of silica nanofluid on the surfaces with higher roughness. As the increment of nanofluid mass concentration from 0.025% to 0.1%, a further reduction of heat transfer coefficient was observed. For the super hydrophobic surface with higher roughness (contact angle 153.0°), boiling heat transfer was enhanced at heat flux less than 93 kW/m^2, and then the heat transfer degraded at higher heat flux.

ARTICLE HISTORY
Received 17 September 2017
Accepted 30 June 2018

KEYWORDS
Super hydrophilic; super hydrophobic; pool boiling; heat transfer

Introduction

As a highly efficient heat transfer method, boiling has been widely used in engineering applications. For energy and material saving considerations, the enhancement of boiling has been one of the primary focuses in the field of heat transfer. In recent years, with the rapid development of compact heat exchanger and micro electromechanical technology, the heat dissipation requirement is more prominent. As a result, many scholars have been dedicated to investigating the effects of changing medium or modifying the surface on pool boiling.

As an effective way to change the characteristics of working medium, addition of nanoparticles into the base solution has been adopted to improve the boiling heat transfer performance[1]. Karimzadehkhouei et al. [2] investigated the nucleate pool boiling heat transfer of TiO_2 nanoparticles/water and CuO nanoparticles/water. It was found that nanoparticle mass fraction corresponding to the best pool boiling performance was highly dependent on the type of nanoparticles. Ham et al. [3] studied the influence of surface roughness on the boiling characteristics of nanofluid. It indicated that the performance of boiling heat transfer for Al_2O_3 nanofluid was closely related to the surface roughness and concentration of nanofluid. Quan et al. [4] investigated the wettability effect of nanoparticles on the bubble behavior and the morphologies of nanoparticles deposition layers. It was shown that nanofluid containing moderate hydrophilic nanoparticles could enhance boiling heat transfer at nucleate boiling regime, but nanofluid containing strong hydrophilic nanoparticles deteriorated the heat transfer. Kiyomura et al. [5] studied the effect of Fe_2O_3 nanoparticles deposition on the pool boiling heat transfer of water. The highest heat transfer coefficient was obtained for the smooth surface with lower nanoparticles mass concentration. Other nanoparticles, such as SiO_2 [6, 7], ZnO[8], ZrO_2[9], Cu[10, 11], and carbon nanotubes (CNT)[12–15] have also been investigated in the literature.

CONTACT Wen-Tao Ji wentaoji@xjtu.edu.cn

Color versions of one or more of the figures in the article can be found online at www.tandfonline.com/umte.

However, so far there is no final conclusion about whether nanofluids can enhance or weaken the pool boiling heat transfer. It depends on many factors like nanoparticle material, surface roughness, volume/mass fraction, particle diameter, and base fluid type. Roughness is also one of the important factors that has effect on the boiling heat transfer. The surface roughness in the literature is mostly in the range of 0.01 to 3μm [3–5, 7, 8, 14]. A higher surface roughness value in the range of 3.9 ~ 6.0μm was tested in the present work.

The characteristics of boiling surface such as wettability can also have significant effects on pool boiling heat transfer. As early as 1902, Boys [16] recorded the superhydrophobic phenomenon "water sprinkled on Clubmosses membrane can spontaneously form spherical droplets and roll freely on the surface". In 1997, Wang et al. [17] reported the TiO_2 super hydrophilic surface (contact angle close to 0 degree) for the first time. Nowadays, many manufacturing technologies of super hydrophobic and hydrophilic surfaces have been developed, such as mechanical processing, laser etching, vapor deposition, and sol-gel method. Yu et al. [18] used the methods of high speed wire cut electrical discharge machining technology and solution immersion to develop a micron level aluminum base super hydrophobic surface with anisotropic V-type groove array, and investigated the effect of groove size on surface wettability.

Hydrophilicity of surfaces can improve the critical heat flux of boiling heat transfer effectively[19–21], and the hydrophobicity can reduce the wall superheat of initial boiling stage[22–25]. Single bubble dynamics in water boiling process was studied on hydrophobic and superhydrophobic surfaces[26, 27]. Hendricks et al. [28] deposited a layer of Zinc oxide nano structure on aluminum and copper surfaces by using microreactor assisted nanomaterial deposition technology. Heat transfer coefficient improvement for nanostructured surface was up to 10 times higher than "bare" Al substrate. The critical heat flux (CHF) of 82.5W/cm^2 with water as fluid for ZnO nano structure on Al was observed versus a critical heat flux of 23.2W/cm^2 on bare Al surface with the wall superheat reduction of 25–38°C. Forrest et al. [29] prepared three types of nanoparticle thin-film coatings including hydrophilic, superhydrophilic and hydrophobic using a layer-by-layer assembly method. Nickel wires coated with different thin films demonstrated significant enhancement in pool boiling. Up to 100% enhancement of the critical heat flux and over 100% enhancement of the heat transfer coefficient were observed. It was concluded that the nanoporous structure coupled with chemical constituency of those coatings led to the enhanced boiling behavior. Pool boiling experiments with degassed water were performed by Bourdon et al. [30] on highly smooth glass substrates to investigate the effect of wettability on onset of nucleate boiling (ONB). The onset of nucleate boiling was observed after superheat of 3.5°C on the hydrophobic surface and the heat transfer coefficient increased suddenly from 1.5kW/m^{2}K to 4kW/m^{2}K. But for the hydrophilic surface boiling occurred until the superheat above 37°C. Shi et al. [31] experimentally investigated the boiling heat transfer of deionized water on the surface of nanowire arrays. Compared with smooth surface, the heat transfer coefficient and critical heat flux of super hydrophobic surface were significantly improved because of capillary force and increased nucleation density on nanowire surface. Fan et al. [32] investigated the transient pool boiling heat transfer performance of water by quenching method under the atmospheric pressure on different wetting surfaces, from superhydrophilic to superhydrophobic. It was observed that film boiling was the main boiling mode for the superhydrophobic surface. The cooling rate during quenching was shown to monotonously accelerate with the increasing of surface hydrophilicity. Boiling heat transfer enhancement, with critical heat flux increasing up to nearly 70%, was achieved for the superhydrophilic surface compared to the hydrophilic case.

With the further investigation on the phase change heat transfer outside super wettability surfaces, recent study is turning to the inhomogeneous wetting surfaces such as biphilic surfaces [33–35]. Zupančič et al. [36] developed a super hydrophilic/hydrophobic structure on the stainless steel by laser pulse technology. It was found that the biphilic surface could not only enhance the heat transfer coefficient, but also greatly improve the critical heat flux. Meanwhile, experimental results also indicated that there was a specific operating condition in which the chemical and mechanical

heterogeneous surface would achieve an optimal performance. According to the investigation of Jo et al. [37], the heterogeneous wettability surface composed of hydrophobic dots on a hydrophilic surface also provided higher nucleate boiling heat transfer coefficient than a homogeneous wettability surface (hydrophilic or hydrophobic). The improvement of boiling heat transfer seemed to be related with the effects of the number of dots, the size of dots, and the pitch between dots. Betz et al. [38] found the largest heat transfer coefficient was obtained on biphilic surface, which was achieved by juxtaposing the hydrophilic and hydrophobic regions. An analytical model was developed to describe how biphilic surface effectively regulating the vapor and liquid transport, delaying critical heat flux and maximizing the heat transfer coefficient.

The strengthening or weakening of the heat transfer coefficient and critical heat flux may be attributed to the following two reasons: hydrophilicity of surfaces can enhance the capillary effect and improve the critical heat flux of boiling heat transfer effectively[19–21]; and the hydrophobicity can increase the number of activated core and reduce the wall superheat at initial boiling stage[22–25]. The combination of hydrophobic and hydrophilic regions may also lead to increase of heat transfer coefficient[33–38]. However, these experimental results and conclusions are obtained under the small surface roughness, most of which is in nanoscale for the resent studies[26–34, 39].

Although many studies have been done on pool boiling heat transfer with different surface wettability and fluids, previous experimental results and conclusions were still partially inconsistent and far from adequate. Even for the same nanoparticle, both enhancement and deterioration were observed [3, 8]. For different hydrophobic [37, 38] and superhydrophobic [34, 38] surfaces with the same wettability, the effects on boiling heat transfer were also different. The chief objective of this article is to investigate the pool boiling heat transfer on the surface with higher roughness and different wettability. Nanofluid is also investigated for comparison. It may also help to facilitate a deeper insight into the mechanisms of pool boiling heat transfer.

In this study, a pool boiling heat transfer test rig was built. Pool boiling heat transfer on higher roughness surfaces with different wettability was conducted with deionized water and silica based nanofluid. The heat transfer performances on different horizontal flat surfaces were presented and compared with the pure copper surface. And the rest of the paper is organized as follows. In Section 2, experimental apparatus and procedure are introduced, including the test rig, preparation of boiling mediums and surfaces, experimental procedure, data reduction and uncertainty analysis, and validation of the experimental system. The results and discussion are provided in Section 3. Finally some conclusions are summarized in Section 4.

Experimental apparatus and procedure

Experimental apparatus

The experimental test apparatus was designed to carry out pool boiling heat transfer experiment at the atmospheric pressure (Figure 1). It mainly consists of the vessel, test sample, electric heating, condensing, and data acquisition system. The vessel for boiling has the internal diameter of 300 mm and 505 mm in height. The wall thickness is 6 mm. The vessel is well insulated with rubber plastic (60 mm) and aluminum foil to prevent the heat loss. Two sight glasses with diameter of 80 mm are configured in the vessel to observe the boiling process. The test sample is a copper block, which has the dimension of 100 mm × 50 mm × 70 mm (length × width × height). The top of the sample is the surface for modification and boiling, and the bottom is in contact with the electric heater with thermal grease. The bottom of copper sample is located in just the middle of the electricity heating block. The other surfaces are wrapped with insulating materials to prevent heat loss from the bottom to top. The insulating materials include high temperature resistant (up to 250 °C) epoxy resin adhesive (10 mm thick) and polytetrafluoroethylene tapes (at least 20 mm). Underneath of the test sample is the electrical heating plate. The size of the plate heater is 150 mm (long) × 150 mm (width) × 15 mm (height). The heating power can be regulated from 0 to 2 kW. The power can be measured

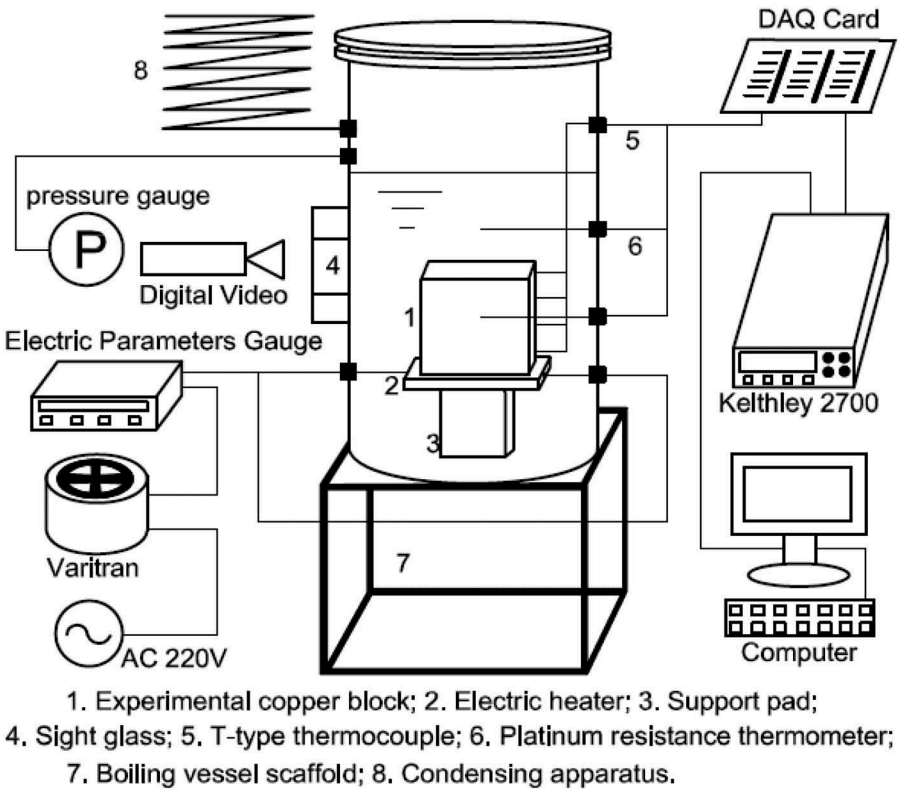

Figure 1. Experimental test rig.

by dynamometer with accuracy of 0.5%. Two auxiliary heaters with maximum power of 2kW are also fixed in the vessel, which are used to promote the pool boiling to reach the saturate state. When the liquid in the vessel reaches the saturate state, it will be turned off. A supporting plate is configured between electric heater and vessel.

In the experiment, electric heater heats the copper block through the bottom by adjusting the voltage regulator. Then the fluid such as deionized water or nanofluid boils and converts to vapor at the atmospheric pressure. The vapor condenses in the condensing unit and the condensate flows back to the boiling pool. The condensing apparatus is cooled by air and made by finned tube. It is connected with the external atmospheric environment. In order to accurately calculate the temperature and the heat flux on the heating surface, 12 T-type copper constantan thermocouples with the precision of ± 0.2K are inserted into the very small holes along the sample copper block (Figure 2). The diameters of the holes are 3 mm and the depths are 25mm. The diameters of thermocouple wires are 0.2 mm. Using a copper rod with diameter of 2.8 mm, the thermocouple wires are pushed and firmly attached to the upper surfaces of the small holes. The thermocouple wires should be kept straight forward when entering the small holes. The position should be accurately fixed and winding is not allowed in the mounting process. The distance between the two neighboring thermocouples is finally measured with micrometer. Three platinum resistances temperature transducers (PT100), which have a precision of ± $(0.15 + 0.002|t|)$ K in the whole test range, are installed in the boiling pool to measure the temperature of the boiling liquid. The atmospheric pressure is measured with a mercury barometer. A Keithley digital voltmeter (Keithley 2700) with resolution of ± 0.1 μV is used to measure the electric potential of thermocouples and resistances of PT100.

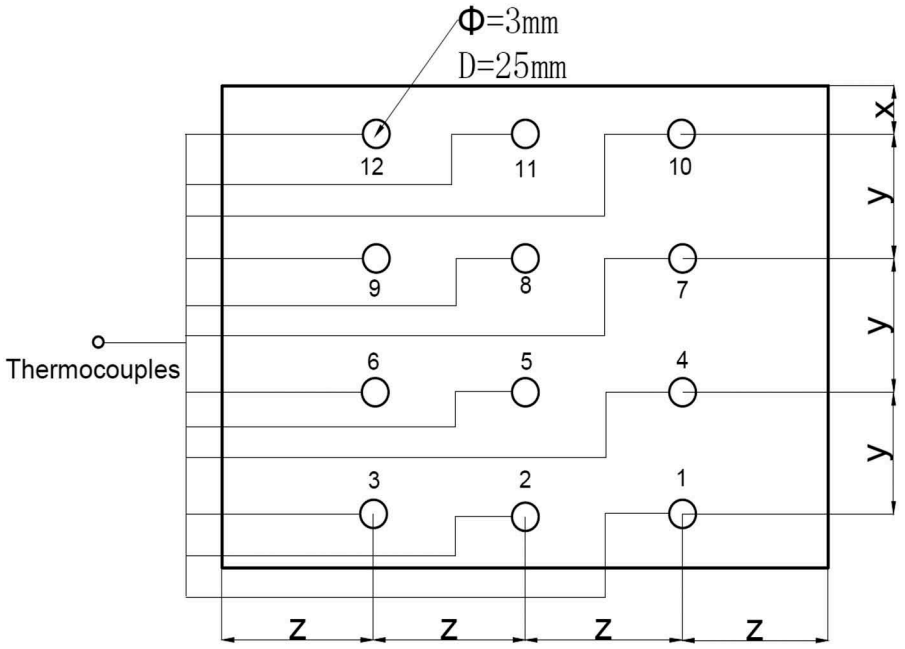

Figure 2. Mounting position diagram of thermocouples in copper block.

Preparation of boiling mediums and boiling surfaces

The boiling mediums included two species: deionized water (DI-W) and SiO_2-water nanofluid (Si-NF). Their thermo-physical properties relevant to this study are summarized in Table 1. The boiling surfaces included: 120# sand cloth polished surface (SPS1), 360# sandpaper polished surface (SPS2), one etched surface by etching solution (ES), two hydrophobic surfaces (HBS1, HBS2), and one superhydrophobic surface (SHBS). Detailed instructions for boiling working fluids and boiling surfaces are shown in the following Table 2. The methods for preparing these boiling fluids and surfaces are described further below.

The resistivity of deionized water was greater than 0.5 MΩ· cm. It was chosen for pool boiling experiment to verify the reliability of the test rig. The results were compared with other experimental data on different surfaces for different boiling fluids. In the experiments, different concentrations of silica nanofluid were also prepared. It included mass concentration of 0.025%, 0.05%, and 0.1%. The molecular weight of silicon dioxide nanoparticle is 60.08 g/mol and the

Table 1. Thermo-physical properties of deionized water and SiO_2 nanofluid at the atmosphere pressure (95.7kPa).

Property	Value
Deionized-water	
Saturation temperature T_s (°C)	98.205
Liquid density ρ_l (kg/m^3)	959.64
Vapor density ρ_v (kg/m^3)	0.5664
Liquid dynamic viscosity μ_l (mN· s/m^2)	0.2883
Thermal conductivity λ_l (W/m· K)	0.6825
Liquid specific heat c_{pl} (J/kg K)	4217.85
Latent heat of evaporation h_{fg} (kJ/kg)	2261.77
Liquid surface tension σ_l (N/m) × 10^{-4}	591.94
SiO_2 nanofluid	
Molecular weight of silicon dioxide nanoparticle (g/mol)	60.08
SiO_2 particle diameter d_p(nm)	30
The purity of SiO_2 particles (metals basis)	99.5%

Table 2. Details for boiling working fluids and boiling surfaces.

Shorthand description		Materials and methods	Boiling liquid
DI-W	Deionized water	Purchased	-
Si-NF	SiO_2-water nanofluid	30 nm hydrophilic SiO_2 nanoparticles and deionized water; One-step method	-
SPS1	Sand cloth polished surface	120# fine horse brand abrasive cloth; Carefully polishing	DI-W, Si-NF
SPS2	Sandpaper polished surface	360# sail brand waterproof abrasive paper; Carefully polishing	DI-W, Si-NF
ES	Etched surface	Livingston etching solution; Dislocation etching method	DI-W
HBS1	Hydrophobic surface	Hydrophobic SiO_2 nanoparticles; Hot press particle sintering	DI-W
HBS2	Hydrophobic surface	Hydrophobic SiO_2 nanoparticles and epoxy resin; Hot press particle sintering	DI-W
SHBS	Superhydrophobic surface	Parylene powder; Vapor phase deposition method	DI-W

particle diameter is around 30 nm. It is hydrophilic and the purity is more than 99.5% (metals basis). The mass of the nanofluid particles was measured by quality meter with a resolution of ± 0.01 g. The charge volume of liquid to the vessel for boiling was around 18 L. The nanofluid was prepared by the following steps: firstly, nanoparticles and deionized water were mixed while stirred with a glass rod in a large beaker (no dispersant or surfactant was added in experiment); then, the mixed suspension was oscillated in a digital controlled ultrasonic vibrating instrument (KQ-500DE type, 220V50Hz) for 5 hours to maintain the stability of nanoparticles suspension in the base fluid. Take a 10-minute break after per hour of oscillation to prevent the overheating of nanofluid. The temperature of ultrasonic cleaning instrument was controlled within 45°C. The ultrasonic vibration power was 500 W.

120# fine horse brand abrasive cloth and 360# sail brand waterproof abrasive paper were used to polish the pure copper surface, respectively. Before polishing, the pure copper was cleaned with deionized water, and then dried by hot air jet. Next, the boiling surfaces were carefully polished by 120# sand cloth (SPS1) and 360# sandpaper (SPS2), respectively. After that, surfaces were rinsed with deionized water and dried by air jet again. The two surfaces were both hydrophilic. Another hydrophilic surface was made by chemical etching (ES). A total of 2096.9 mL deionized water, 2.3 mL hydrochloric acid with a mass concentration of 37%, and 0.8 mL glacial acetic acid with a mass concentration of 99.5% were sequentially poured into the beaker and slowly stirred with glass rod at the same time to prepare the Livingston reagent. Then the hydrophilic surface polished by 360# sandpaper was immersed in the Livingston solution at ambient temperature (about 2–14°C) for 17 hours to implement dislocation etching. After etched sample was cleaned by deionized water and dried in vacuum drier at 80°C, the contact angle reduced to 41.4 degrees, which became more hydrophilic than the untreated surface.

Hydrophobic surfaces were prepared by two methods. The first one (HBS1) was developed by sintering hydrophobic nanoparticles on the boiling surface of copper block. First, a thin layer of hydrophobic silica nanoparticles film was uniformly spread on the boiling surface, and then the surface was pressed with a pressure of about 40 kPa and temperature of about 200 °C for 95 min. A long sintering process was beneficial to increase the coating layer's durability. The contact angle increased to 123.8 degrees after the hot press sintering process. The molecular weight of fumed silicon dioxide used to sinter is 60.08 g/mol and the particle size is 7–40 nm. Specific surface area is 100 m^2/g. The nanoparticles are hydrophobic and the purity is greater than 99.8% (metals basis). The second hydrophobic surface (HBS2) was obtained with a thin layer of hydrophobic nano-silica and epoxy resin mixture sintered outside the boiling surface. The sintering conditions were the same as above. The mixing of hydrophobic nanoparticles and epoxy resin made the adhesion of the coating on the boiling surface more durable. Consequently, the contact angle rose up to 134.4 degrees after bonding of the mixture.

Super hydrophobic surface (SHBS) was developed with Parylene vapor phase deposition method. The process of Parylene deposition was as follows: Parylene powder was firstly heated in the vacuum oven (150°C) and changed into vapor; then it was cracked in the high temperature furnace (650–700°C) and changed into reactive macromonomer; finally the vapor macromonomer deposited in the solid surface in the ambient-temperature (35°C). Pure copper surface was firstly polished by 120# sand cloth, and then a layer of Parylene film was deposited on the surface through vapor-phase deposition method. The contact angle of 153.0 degrees was obtained finally.

Experimental procedure

The pool boiling heat transfer was tested on six higher roughness boiling surfaces with different wettability, and for two mediums with discrepant properties. All boiling heat transfer experiments were conducted under saturated condition at the atmospheric pressure close to 96kPa. After the fluid was charged into the boiler, it was then preheated to the saturated temperature with two pre-heaters. Prior to each experimental test, the working fluid in saturated state was kept boiling for 30 minutes to drain the noncondensable air in the container. The voltage regulator could regulate the electric voltage from 0 to 240 V and the experiments were carried out by gradually increasing the electrical load until the maximum voltage was reached.

In experiments, the data were recorded by Keithley 2700 every 100 seconds for a loop. When all test data were stable, they were saved and the heating power was steadily adjusted to the next measuring point. During the tests, the range of heat flux was 30–300kW/m^2 and the heating power was stepwise increased. The criterion for steady state was that the temperature fluctuation of boiling liquid and copper block was within ± 0.1 K, mostly within ± 0.05 K. The measurement of the pool boiling curve for deionized water on pure copper surface at the atmosphere was repeated twice and good reproducibility was obtained. Hence the later boiling process was measured only once.

Data reduction and uncertainty analysis

The heat flux was calculated according to Fourier's law assuming 1-D heat conduction along the upward direction of copper block. Boiling surface temperature was determined by extrapolating the linear temperature profile to the block upper surface. The wall temperature data were measured from the thermocouples embedded in the test sample block. Twelve holes were punched on the back of copper block and thermocouples were installed in the positions as Figure 2. x was the distance between the top row of thermocouples from the upper boiling surface. y was the spacing between adjacent two rows of thermocouples, and z was the spacing between adjacent two columns. x, y and z were 5 mm, 20 mm and 25 mm respectively. The accurate values were measured with slide micrometer.

In the experiment, copper block was well insulated and the temperature exhibited an almost linear trend in the heat transfer direction. Standard linear regression can be performed. Take the pool boiling heat transfer of deionized water on 120# sandpaper polished surface as an example, inner surface temperature fitting curves for different heat fluxes were obtained as Figure 3. The abscissa was the distance from the bottom of the copper block. Vertical axis was the average temperature at the positions where the thermocouples were placed. Average temperature was the average value of three thermocouple readings on the same column. The R-squares of curve fittings were always higher than 0.99. As shown in Figure 3, the temperature decreased linearly with increasing of distance. Hence, 1-D Fourier's heat conduction law and linear extrapolation were adopted to obtain the heat flux and boiling surface temperature.

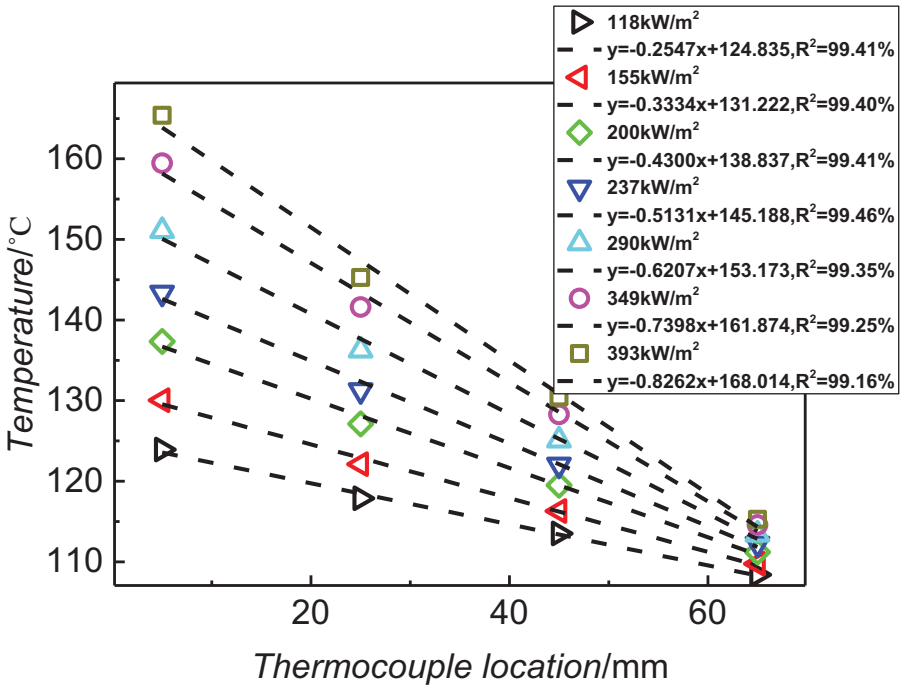

Figure 3. Temperature linear fitting curves at different heat flux for deionized water pool boiling on 120# polished surface.

The heat flux through boiling surface was calculated as followed:

$$q = \lambda \cdot \frac{\partial T}{\partial y} = \lambda \cdot |k| \tag{1}$$

where λ is thermal conductivity of copper, k is the slope of the best temperature linear curve. Consequently, the boiling surface temperature T_w was calculated with the following equation:

$$T_w = \frac{T_{10} + T_{11} + T_{12}}{3} - \frac{q}{\lambda} \cdot x \tag{2}$$

where T_1, $T_2, \cdots T_3$ are temperatures corresponding to holes $1, 2, \cdots, 12$, respectively. The boiling heat transfer coefficient h was obtained using the Newton's law of cooling:

$$h = \frac{q}{T_w - T_s} \tag{3}$$

where T_s is the saturated temperature corresponding to local atmospheric pressure, which was measured by PT100.

According to [40], the uncertainty analysis has been conducted to estimate the possible uncertainty of experimental data and the reduced results. The confidence levels for all measurements are within 95%. Based on the linear curve fittings, errors of temperature and distance measurements, the estimated uncertainties of heat flux q through the boiling surfaces are within 4.46%. The uncertainties of boiling surface temperature are lower than 4.48%. The error bars are also shown in the figures. As shown in the figure, the largest deviation occurs in the highest heat flux. And the uncertainties of boiling heat transfer coefficient h are less than 6.32%.

Validation of the experimental system

The pool boiling heat transfer of deionized water on copper surface was tested at the atmospheric pressure. And the experimental result was compared with Rohsenow correlation [41], which was given as follows:

$$\frac{c_{pl}\Delta t}{h_{fg}} = C_{wl}\left[\frac{q}{\mu_l h_{fg}}\sqrt{\frac{\sigma_l}{g(\rho_l-\rho_v)}}\right]^r \mathrm{Pr}_l^s \ (s=1;\ r=0.33) \tag{4}$$

where μ_l, h_{fg}, c_{pl}, and Pr_l are the liquid viscosity (kg/m· s), the latent heat of vaporization (kJ/kg), the liquid specific heat (kJ/kg· K), and the liquid Prandtl number, respectively. q is the heat flux of nucleate pool boiling. C_{wl} is the empirical parameter depending on the combination of fluid and surface. $C_{wl} = 0.013$ was adopted here for the pure copper surface.

Figure 4 shows the comparison of experiment measurements and Rohsenow correlation at different heat fluxes. The heat transfer coefficient is plotted against heat flux in double logarithmic graph. The relative deviation of experimental results from Rohsenow correlation lies within −4.39% and 18.3% at the heat flux range from 30 kW/m^2 to 300 kW/m^2. The comparison should validate the accuracy and reliability of experimental apparatus and procedure.

Results and discussion

Boiling surfaces characteristics

The Bruker GT-K white light interference microscope was adopted to measure the surface roughness of heating surface. Roughness on different boiling surfaces before and after pool boiling experiments was presented in Tables 3 and 4. A typical area with size 9mm× 8mm was

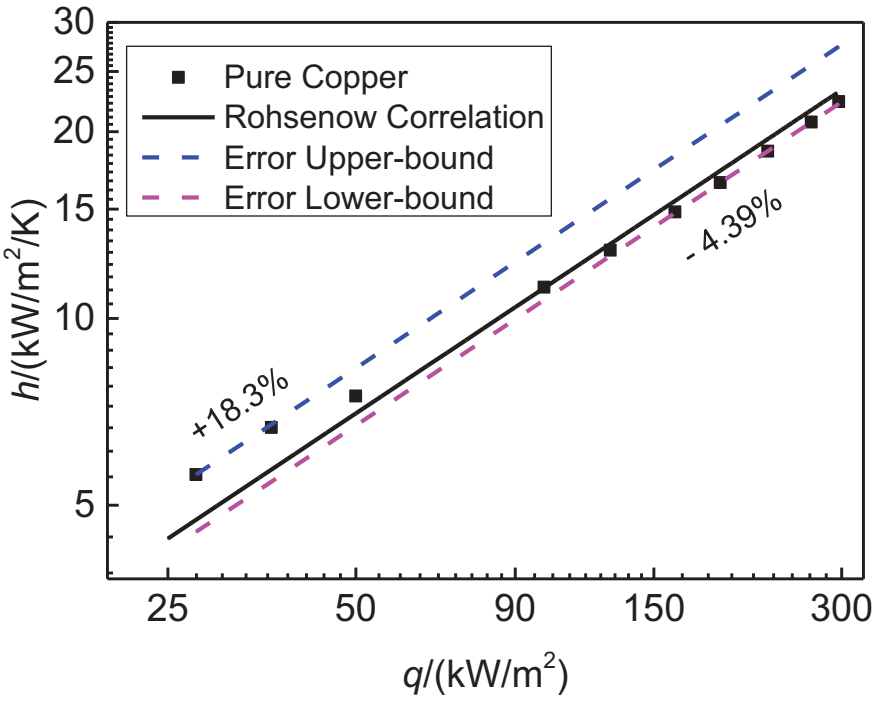

Figure 4. Comparison of deionized water pool boiling heat transfer coefficient with Rohsenow correlation.

Table 3. Roughness of sandpaper polished boiling surfaces measured by the GT-K white light interference microscope.

Surfaces roughness			*Ra*, μm (arithmetic average roughness)		*Rt*, μm (total height of profile)	
Boiling surfaces	Boiling mediums		Before boiling	After boiling	Before boiling	After boiling
120# polished surface(SPS1)	SiO_2-DI nanofluid	0.025%	3.903 ± 0.276	5.893 ± 0.141	209.739 ± 2.497	188.308 ± 2.544
		0.05%		5.589 ± 0.134		195.122 ± 2.499
		0.1%		3.843 ± 0.095		170.28 ± 2.43
360# polished surface(SPS2)	SiO_2-DI nanofluid	0.025%	5.938 ± 0.25	5.072 ± 0.176	175.385 ± 2.538	153.148 ± 2.528
		0.05%		6.707 ± 0.203		97.458± 1.822
		0.1%		5.667 ± 0.183		98.95 ± 1.6

Table 4. Roughness of different wettability boiling surfaces measured by the GT-K white light interference microscope.

Surfaces roughness		*Ra*, μm (arithmetic average roughness)	*Rt*, μm (total height of profile)
Boiling surfaces	Boiling mediums	Before boiling	Before boiling
Etched surface (ES)	Deionized water(DI)	4.791 ± 0.224	152.469 ± 2.697
Hydrophobic surface1 (HBS1)	Deionized water(DI)	4.427 ± 0.180	216.515 ± 1.734
Hydrophobic surface2 (HBS2)	Deionized water(DI)	4.561 ± 0.206	224.656 ± 1.931
Superhydrophobic surface(SHBS)	Deionized water(DI)	4.135 ± 0.167	211.314 ± 1.634

chosen as the measuring field, which was located in the middle of the boiling surface. And if the results of successive measurements were close, the average value was taken as the measurement value of roughness. Otherwise, it would be retested. The standard deviation of the measurement was also shown in Tables 3 and 4. The largest deviation of surface roughness was within ± 2.697μm. Arithmetical mean roughness *Ra* is the arithmetical mean of the absolute values of the profile deviations from the mean line of the roughness profile. Total height *Rt* of the roughness profile is the difference between height of the highest peak and depth of the deepest valley within the evaluation length.

As shown in Tables 3 and 4, 360# sandpaper polished surface had larger *Ra* and smaller *Rt* values than 120# sand cloth. Larger *Ra* meant that the surface had greater average roughness, while smaller *Rt* meant that peak height and valley depth on boiling surface were more uniform. The measurement results also showed that there was virtually no regular variation trend in superficial arithmetic average roughness *Ra* before and after nanofluid pool boiling experiments. It indicated that nanoparticles distributed evenly across the surface micro cavities in boiling. In this paper, the size of SiO_2 nanoparticles is 30nm and the surface roughness is in micron scale. In other words the ratio of particles size to roughness (d_p/Ra) is far less than 1. Hence the original rough pits would be covered with tiny nanoscale SiO_2 particles and thus the surface structure changed. For nanofluid pool boiling, the total height *Rt* of profile decreased slightly after boiling. And with the increase of the concentration of nanoparticles, the total height of profile *Rt* decreased. The decline was because small gaps on the boiling surface were gradually filled with nanoparticles in the experiments. Arithmetic average roughness *Ra* and total height of profile *Rt* of the etched surface were both lower than 360# polished surface. Two kinds of roughness for hydrophobic and superhydrophobic surfaces were both higher than that of 120# polished surface.

Static contact angles of liquid drop on the six higher roughness boiling surfaces are shown in Tables 5 and 6. An Attension Theta contact angle analyzer and optical measurement software (OneAttension control software) were used to measure the static contact angle of deionized water and nanofluid on the six boiling surfaces before and after boiling experiments. All contact angle measurements were carried out at the room temperature and the average value of more than 50 measurements was finally adopted. The standard deviation of the measurement values was shown as error bar in Tables 5 and 6. The largest deviation of contact angle was within ± 3.2°. Characterization of the hydrophilic, superhydrophilic, hydrophobic, and superhydrophobic surfaces are shown in Figures 5 and 6. It include the static, advancing, and receding contact angles. SEM images of the

Table 5. Static contact angle of liquid drop on the sandpaper polished boiling surfaces.

Static contact angle(SCA)/°			SCA of water drop on the surface		SCA of nanofluid drop on the surface
Boiling surfaces	Boiling mediums		Before boiling	After boiling	After boiling
120# polished surface(SPS1)	SiO_2-DI nanofluid	0.025%	58.6 ± 2.3	8.1 ± 1.3	3.5 ± 1.8
		0.05%		4.8 ± 0.3	3.3 ± 1.1
		0.1%		5.8 ± 0.7	3.3 ± 0.3
360# polished surface(SPS2)	SiO_2-DI nanofluid	0.025%	76.5 ± 0.2	10.4 ± 1.3	4.7 ± 1.0
		0.05%		9.8 ± 2.3	6.5 ± 1.1
		0.1%		7.1 ± 0.6	6.4 ± 1.0

Table 6. Static contact angle of water drop on the different wettability boiling surfaces.

Static contact angle(SCA)/°		SCA of water drop on the surface
Boiling surfaces	Boiling mediums	Before boiling
Etched surface (ES)	Deionized water(DI)	41.4 ± 1.9
Hydrophobic surface1 (HBS1)	Deionized water(DI)	123.8 ± 3.2
Hydrophobic surface2 (HBS2)	Deionized water(DI)	134.4 ± 0.9
Superhydrophobic surface(SHBS)	Deionized water(DI)	153.0 ± 0.8

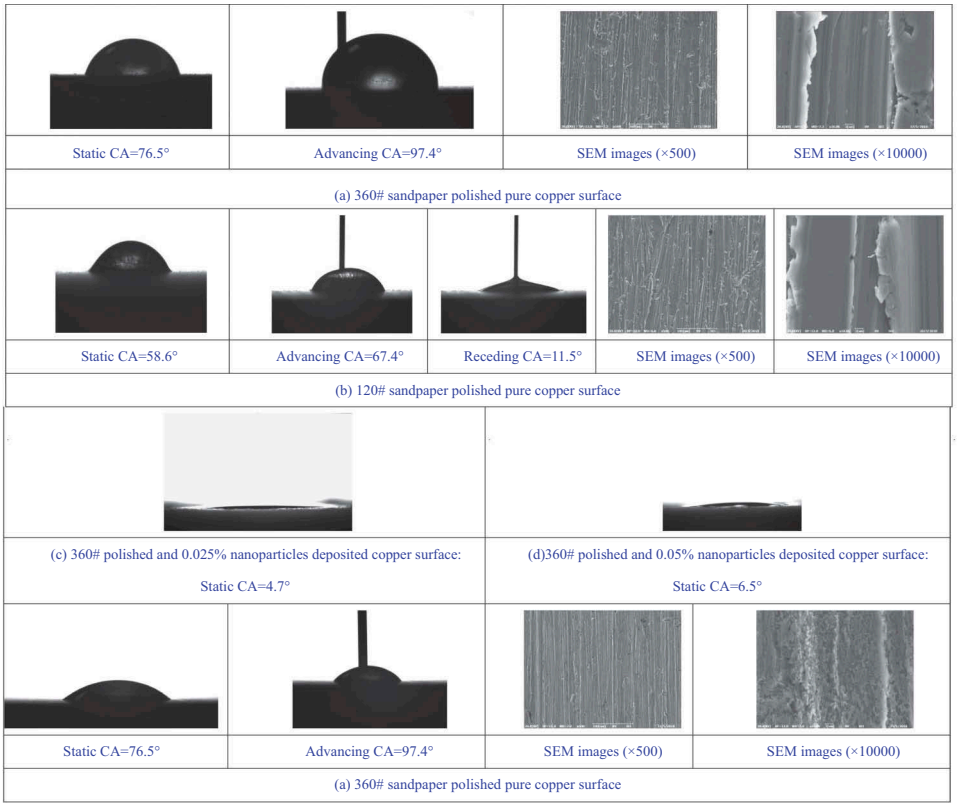

Figure 5. Characterization of the hydrophilic and superhydrophilic surfaces.

surface with 500× and 10,000× magnifications are also shown in the figures. The hysteresis angle is shown in Table 7.

With the increasing of roughness *Ra* from 120# to 360# polished surface, the surface hydrophilic characteristic was weakened, which seemed to be different from the result in [42]. This inconsistency

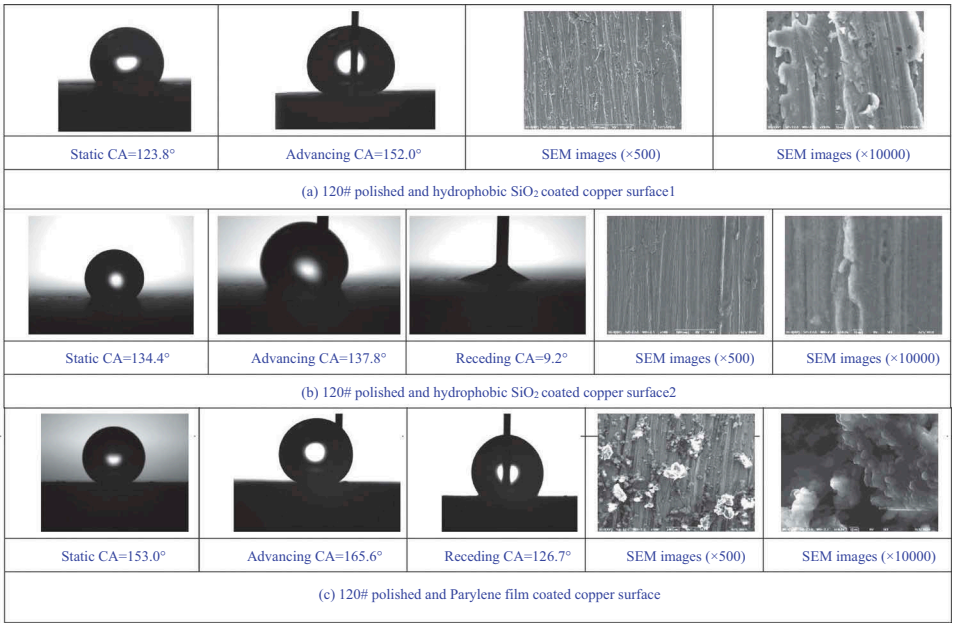

Figure 6. Characterization of the hydrophobic and superhydrophobic surfaces.

Table 7. Hysteresis for the tested surfaces.

Surface	Static CA(°)	Hysteresis(°)
360# sandpaper polished surface	76.4	~ 90.5
360# sandpaper polished and Livingston solution etched copper surface	40.4	~ 40.1
120# sandpaper polished surface	58.6	55.9
Hydrophobic surface 1: 123.3°	123.3	~ 152
Hydrophobic surface 2: 134.4°	134.4	128.6
Superhydrophobic surface	153.0	38.9

was related to the surface structure and morphology difference between 120# sand cloth and 360# sandpaper. After the SiO_2 nanofluid pool boiling experiment, the contact angles of 120# and 360# polished surfaces decreased rapidly and even changed from hydrophilic to ultra hydrophilic. The reason for this trend was the deposition of SiO_2 nanoparticles on boiling surface during boiling. The SiO_2 nanoparticles sediment was hydrophilic and the deposition layer also had porous micro-nano structure, both leading to the super hydrophilic feature of boiling surface. With the increment of nanoparticles mass fraction, contact angle of the deposited surfaces decreased slightly or almost remained in the same level. This implied that the concentration of nanoparticles didn't affect the porous microstructure of the deposited layer on the boiling surface. Compared to 360# polished surface, at the same nanoparticles concentration, the 120# polished surface after nanofluid boiling experiment always showed enhanced feature of hydrophilicity. It was related to the initial roughness of boiling surface. A boiling surface with less initial roughness (*Ra*) might be easier to be uniformly deposited and completely covered with nanoparticles when nanoparticles size was less than the surface roughness by several orders of magnitude. After nanofluid pool boiling experiment on either 120# polished surface or 360# polished surface, static contact angles of nanofluid drop on boiling surface were always less than that of deionized water on boiling surface. This suggested that the surfaces deposited by nanoparticles tended to be closer to nanofluid than deionized water. Compared with 360# sand cloth polished surface, the etched copper surface was more hydrophilic, with the contact angle changing from 76.5°to 41.4°in etching. This was because the dislocations of copper

crystal surface were etched and dissolved by the etching liquid, thus changing the microstructure of the boiling surface.

For the sintered surface 1, the hydrophobicity of the sintered particles, SiO_2, and the porous structure of the surface made the surface to be hydrophobic. For the sintered surface 2, due to the presence of epoxy resin in the sinter layer, more hydrophobic SiO_2 was sintered on the boiling surface, and the hydrophobicity was enhanced. The superhydrophobic surface up to 153° was obtained with a single molecule of gas deposition. The contact angles of two hydrophobic and super hydrophobic surfaces were not measured after the boiling experiments. In the hydrophobic surfaces preparation process, hot pressing temperature was about 200°C and epoxy resin mixture melt temperature was higher than 200°C. They were all higher than the boiling surface temperature in the experiment. However, it was detectable by naked eyes that hydrophobic nanoparticles on boiling surfaces might lose about 30% after the boiling experiments. While, water could still form spherical droplets on the surface after the boiling experiment. Parylene powder has higher strength and good corrosion resistance. After the experiment, the Parylene film on the superhydrophobic surface was still visible and complete to the naked eyes.

To sum up, the finer the preparation process was, and the smaller the controlled scale was, the easier it is to obtain a boiling surface with super hydrophilicity or super hydrophobicity. Through the regulation of the surface, the characteristics of boiling heat transfer might be promoted to the maximum extent.

Pool boiling heat transfer on flat hydrophilic surfaces

The pool boiling heat transfer of deionized water and nanofluid (hydrophilic SiO_2) on three different hydrophilic surfaces with higher roughness was tested at the atmospheric pressure. As indicated above, the pure copper surfaces polished by 360# sandpaper and 120# sand cloth were all hydrophilic. But after the nanofluid boiling experiment the roughed surfaces changed into more hydrophilic even superhydrophilic due to the deposition of silica nanoparticles. Meanwhile, the boiling characteristics also changed. Pool boiling heat transfer experiment results on flat hydrophilic surfaces are shown in Figures 7 and 8. Figure 7 shows the boiling curves of different hydrophilic surfaces. The error bars of pool boiling heat transfer curves of deionized water and nanofluid were also shown in Figure 7. The largest deviation occurs in the highest heat flux. Figure 8 describes the variation of boiling heat transfer coefficient against heat flux on different hydrophilic surfaces. The effects of surface structure and fluid characteristics are described and discussed as follows.

Hydrophilicity of surfaces can improve the critical heat flux of boiling heat transfer effectively [19–21], but this property might not contribute to promoting the early nucleation of bubbles. From Figure 7, the superheat of onset of nucleate boiling (ONB) for SiO_2 nanofluid was 7–10 °C. While for deionized water pool boiling, it was just 5–7 °C. After the nanofluid boiling experiment, the changes in roughness was not evident. The deposition of SiO_2 nanoparticles on boiling surface made the surface to be more hydrophilic, namely, a hydrophilic surface. It delayed the advent of nucleate boiling and increased the initial wall superheat(as shown in Tables 3 and 5). This is also supported by the previous studies in [4, 5, 10]. In the test heat flux range, critical heat flux was not reached for the pool boiling experiment on all flat hydrophilic surfaces with higher roughness in Figure 7.

As shown in Figure 8, the pool boiling of nanofluid generally had lower heat transfer coefficient than deionized water. For deionized water boiling, the surface roughed by 360# sandpaper had the highest heat transfer coefficient than the other two surfaces. It was 25.5% higher than Rohsenow correlation at heat flux of 280 kW/m^2. As the increment of heat flux, the difference between boiling heat transfer coefficient and Rohsenow correlation was increasing. The reason was that the increasing roughness had positive effect on the pool boiling heat transfer. The surface etched by Livingston solution normally had the same heat transfer performance as the surface polished by 120# sand cloth for the deionized water. It was a little bit lower than the Rohsenow correlation. The pool boiling of nanofluid generally had lower heat transfer coefficient than deionized water. For the same sandpaper

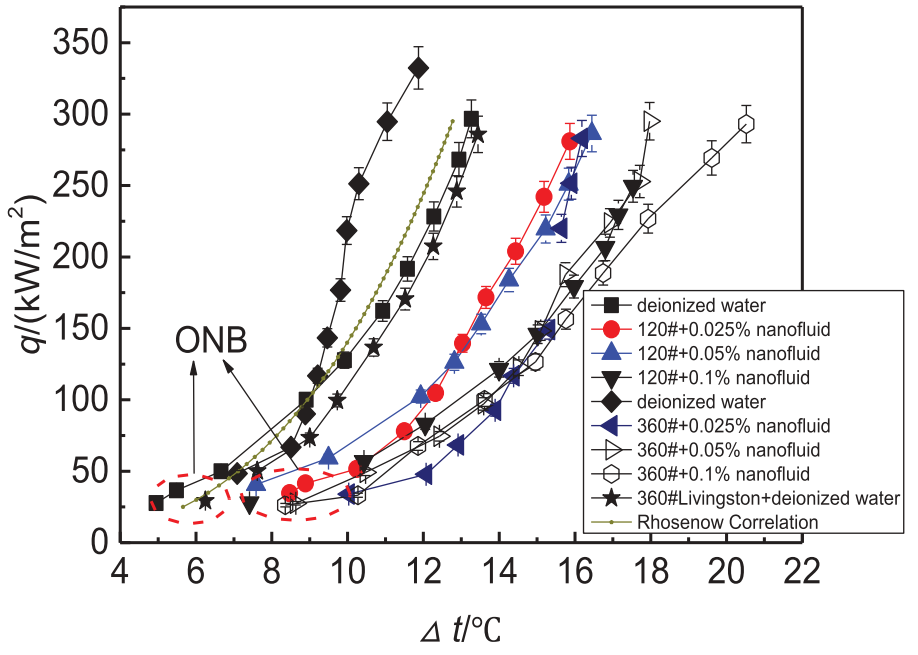

Figure 7. Boiling curves of deionized water and SiO_2 nanofluid on hydrophilic surfaces.

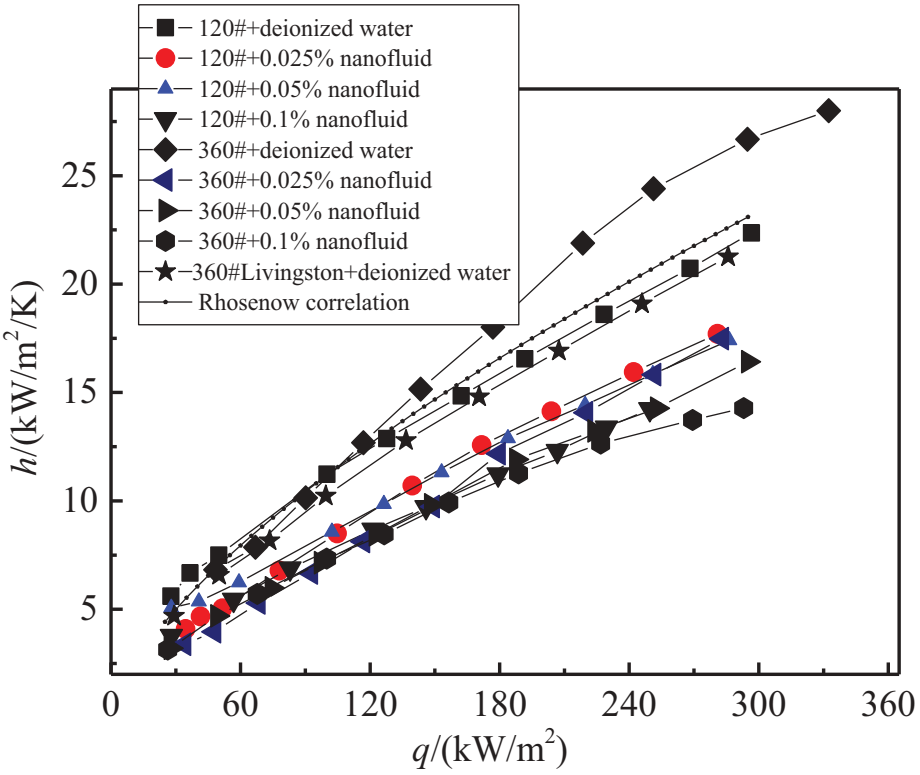

Figure 8. Variation of boiling heat transfer coefficient versus heat flux for deionized water and SiO_2 nanofluid on hydrophilic surfaces.

roughed surface, as the increment of nanofluid concentration, it diminished the pool boiling heat transfer performance. As the concentration increased from 0.025% to 0.1%, the degradation was around 11% for the 120# sand cloth roughed surface; it was up to 22% for the 360# roughed surface. The concentration of 0.05% behaved somewhat in between.

In particular, for the experiment with deionized water, the heat transfer coefficient for 360# sandpaper roughed surface was typically higher than 120# sand cloth roughed case. While, for the nanofluid pool boiling, the heat transfer coefficient of 120# sand cloth roughed surface was higher than that roughed with 360# sandpaper. The two results seemed to be inconsistent. It was speculated that nanoparticles deposition outside the heating surface and the changes of contact angle and surface microstructure were the reasons for the difference. The 360# sandpaper roughed surface for deionized water boiling had larger arithmetic average roughness and static contact angle than 120# surface, which both had a positive effect on heat transfer enhancement [23, 24]. But for nanofluid boiling, the heat transfer coefficient decrement of 360# surface might be caused by the more homogeneous nanoparticles deposition on the boiling surface with lower Rt values.

In order to demonstrate the effect of higher roughness on the deposition of nanoparticles, the schematic diagram of nanoparticles deposition on two typical rough surfaces are given in Figure 9. It is more easily to form homogeneous deposition of nanoparticles for larger Ra and smaller Rt of boiling surface in Figure 9(a) corresponding to 360# polished surface. The mass concentration lines at the same height in Figure 9(a) and (b) represent the equality of the concentration. It can be observed that the surface with lower Ra and larger Rt such as 120# polished surface is not easy to be evenly deposited by nanoparticles. At lower nanoparticles mass concentration, higher peaks outside the surface are directly contacting with the water. As a result, 120# sand cloth roughed surface showed better heat transfer performance than 360# case. It is only a qualitative analysis, the actual conditions in the deposition process should be more complicated.

The decrease of the contact angle could reduce the number of active cavities on the boiling surface according to Yang and Kim [43] as follows:

$$N_a = N_s \int_{R_{\min}}^{R_{\max}} \varphi(R) dR \int_0^{\theta} \theta(\beta) d\beta \tag{5}$$

where N_a is the number of active cavities per unit surface area, and N_s is the cavity areal density. $\varphi(R)$ is the distribution function for the cavity radius, and $\theta(\beta)$ is the cavity opening angle distribution function. $\theta(R)$, $\theta(\beta)$ and N_s are depending on surface microstructure. The rougher and more complex the surface structure is, the larger values of $\varphi(R) \cdot N_s$ and $\theta(\beta) \cdot N_s$ are. $R_{\max}$ and $R_{\min}$ are the maximum and minimum active cavity radii respectively and they are affected by heat

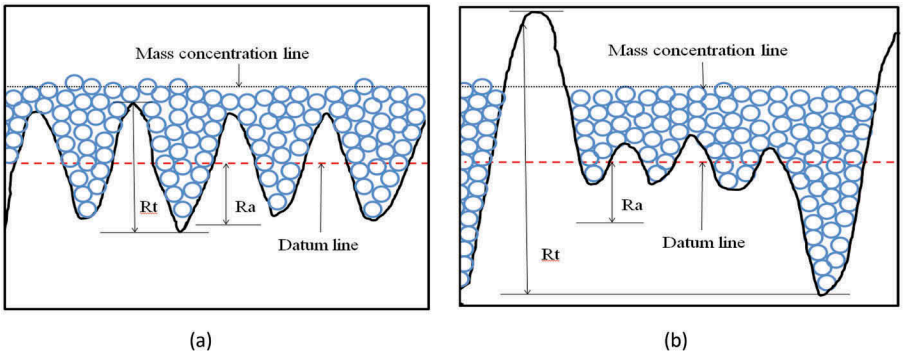

Figure 9. Schematic diagram of nanoparticles deposition on two typical roughed surfaces.

flux. θ is the contact angle of boiling surface. If other variables are kept invariant, N_a will reduce with the decrease of contact angle, thus heat transfer deteriorating. After the nanofluid boiling experiment, one thin layer of nanoparticles were deposited outside the heating surface. The measured surfaces were all changing from normal to more hydrophilic and thus heat transfer deteriorated. Formula (5) was only used as a qualitative analysis here. Distribution functions for the cavity radius and opening angle were not measured in this experiment.

At the same heat flux, with the increase of mass concentration of nanoparticles, the heat transfer coefficient reduction was minor, which was mostly resulted from the adding of thermal resistance of deposited nanoparticles, because the contact angles of these superhydrophilic surfaces almost kept invariant according to Tables 5 and 6. In the boiling process, as the water evaporated, the nanoparticles retained and accumulated in the surface. Hence, as the increment of nanoparticles concentration, the deposit amount and thermal resistance of deposited layer were also increasing, thus the heat transfer performance decayed slightly. Even though the effect was not significant, usually around 1–3%, and not important for engineering design, it might be important for the mechanism analysis. In this paper, for nanofluid pool boiling, the best heat transfer performance was obtained from the boiling process for 0.025% SiO_2 nanofluid on 120# polished surface. It is the smallest mass concentration, smaller *Ra*, and lager *Rt*.

In Figure 10, the experimental result of nucleate pool boiling heat transfer for 30 nm SiO_2-water nanofluid with mass concentration of 0.1% on 120# sand cloth polished surface was compared with the experimental results reported by Liu [44], Milanova [45], Gerardi [46], and Xue [47]. The roughness of surface, nanoparticles size and nanofluid concentration were also showed in the figure. In the five experimental results, Xue's result showed the best heat transfer performance and Milanova's result was the worst. The experimental result in this article was in between. Compared to Liu's result for 35 nm nanoparticles suspension with 0.5% weight fraction, experimental result for 30 nm nanoparticles suspension with 0.1% weight fraction presented in this paper was better.

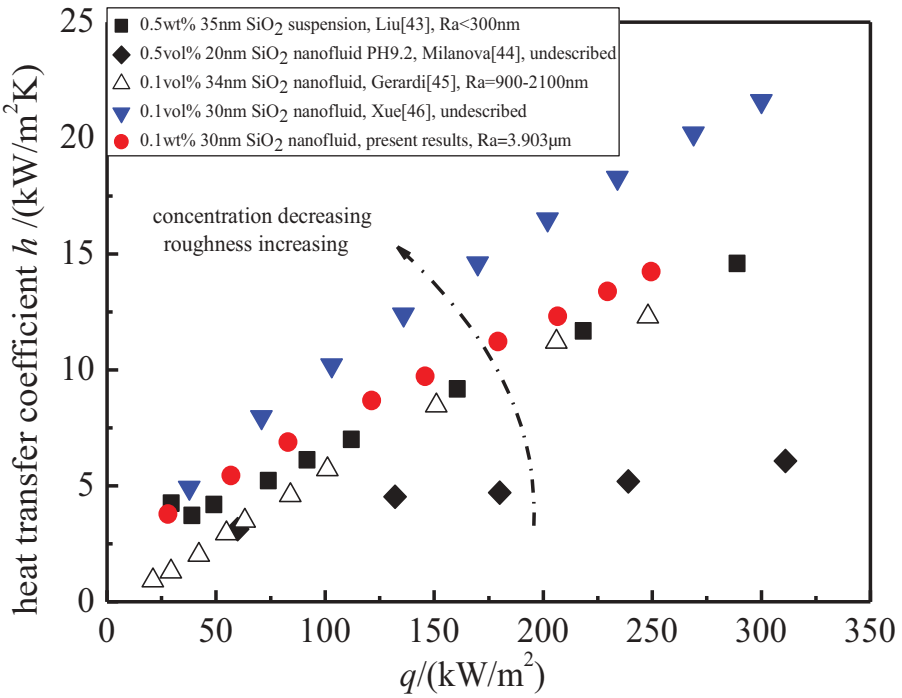

Figure 10. SiO_2 nanofluid pool boiling experiment results at present and that from literature.

In general, the surface structure and contact angle both have an important influence on boiling heat transfer. Greater surface roughness is beneficial to the enhancement of boiling. The decrease of contact angle or the hydrophilization of boiling surface might be unfavorable to boiling heat transfer. However, when the effect of surface structure and contact angle are combined, the influence on boiling heat transfer is rather sophisticated. The changes in roughness not only affect the number of vaporization core and contact angle, but also affect the nucleation process of bubbles according to the principle of bubble dynamics [5]. The deposition of nanoparticles may lead to the decrease of contact angle, but also changes the surface morphology and roughness. The two factors are mutually coupled and further research is needed.

Pool boiling on hydrophobic and superhydrophobic surfaces

The nucleate pool boiling heat transfer experiments on three hydrophobic and superhydrophobic surfaces with higher roughness (4–6μm) were also conducted at the atmospheric pressure. The heat flux ranged from 30kW/m^2 to 300kW/m^2. These hydrophobic and superhydrophobic surfaces were prepared in advance with the aforementioned methods. The contact angles of hydrophobic surfaces are 123.7°and 134.4°, respectively. It is 153.0°for superhydrophobic surface.

Pool boiling curves of deionized water on different wetting surfaces are presented in Figure 11. It was observed that basically the hydrophobic surfaces behaved similarly. Normally, hydrophobic surface had higher heat transfer performance than pure copper in the investigated heat flux. The superhydrophobic surface was more efficient in lower heat flux and the efficiency was decreasing at higher heat flux. It should be noted that the surface added some additional thermal resistance for the very thin layer of coating like hydrophobic SiO_2 film and Parylene. That might also cause the curves to be different from the pure copper surface polished by 120# sand cloth. Compared with hydrophilic surface presented above, to obtain the same heat flux, nucleate boiling on hydrophobic and

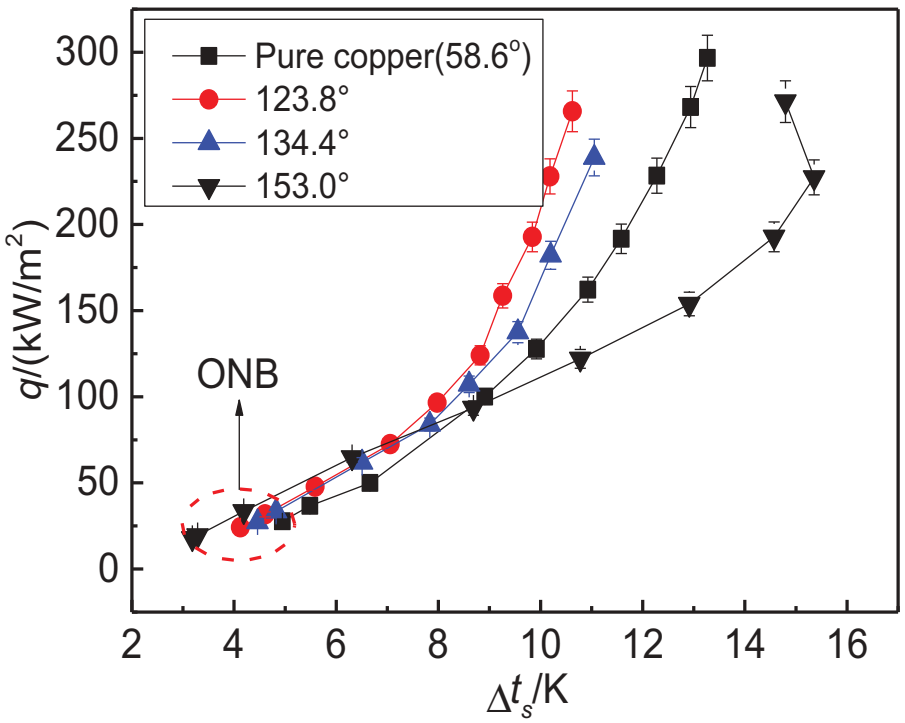

Figure 11. Boiling curves for hydrophobic and superhydrophobic surfaces.

super hydrophobic surfaces required less wall superheat. The onset of nucleate boiling (ONB) was 4–5°C for two hydrophobic surfaces, and close to 3°C for the super hydrophobic surface. It was concluded that hydrophobicity of boiling surface reduced the initial wall superheat of nucleate boiling and such effect was aggravated with the enhancement of hydrophobicity. So they are typically efficient than the hydrophilic surfaces.

In order to express clearly the variation trend of the boiling heat transfer performance, enhancement ratio c (a relative method) was proposed, as shown in Figure 12. The parameter c was defined as the ratio of heat transfer coefficients of various surfaces to the fitting curve obtained from boiling experimental results on pure copper surface. Two hydrophobic surfaces always had better heat transfer performance than the pure copper surface with contact angle of 58.6° in the whole experimental range of heat flux. It might prove that lower wettability had a positive effect on nucleate boiling. With the contact angle increment of hydrophobic surfaces from 123.7° to 134.4°, the boiling heat transfer coefficient enhancement ratio decreased and it might due to the increased thermal resistance produced by epoxy resin. The super hydrophobic surface was special, and further increase in the heat flux had severe effect on the enhancement of heat transfer. The reduction was obvious as the experiment proceeding at the higher heat flux. So when the heat flux was approximately below 93 kW/m^2, the heat transfer coefficient enhancement ratio of super hydrophobic surface reached even more than 2.5. While, as the heat flux passed about 93 kW/m^2, the heat transfer coefficient enhancement ratio was even less than the pure copper surface. Moreover, it was interesting to note that a mild increment after a rapid reduction was both observed as the increment of heat flux for the hydrophobic and super hydrophobic surfaces.

Pool boiling heat transfer outside the surfaces behaves differently depending on both the wettibility and micro-structure of the tested surface. As shown in the SEM images, the structures of the unidirectional scratches can be further modified with the nanoparticle coatings. The scratches of

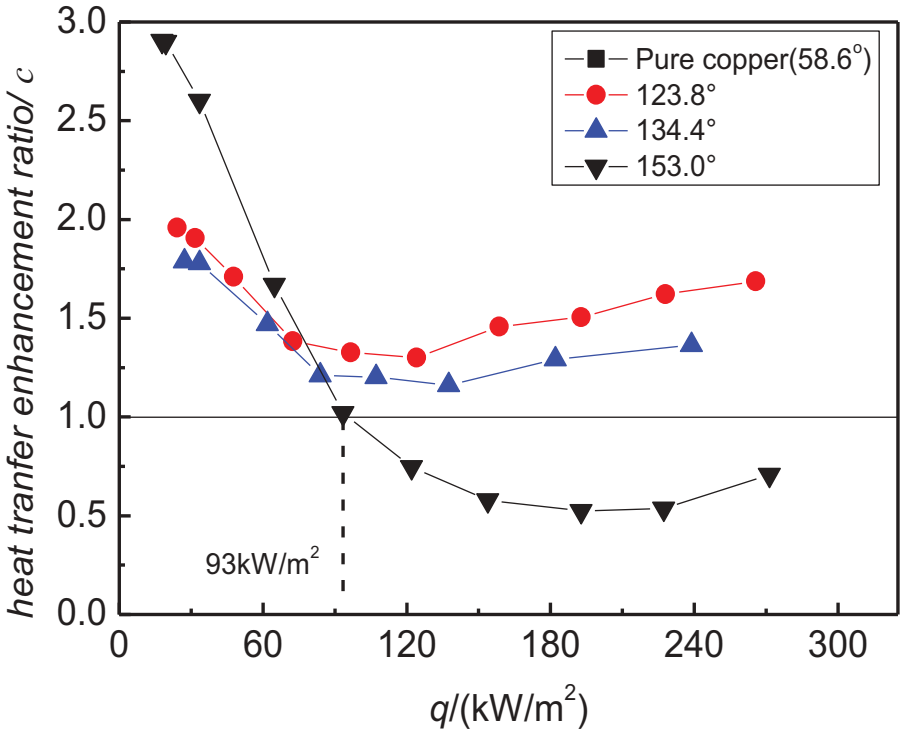

Figure 12. Variation of boiling heat transfer enhancement ratio against heat flux on hydrophobic and superhydrophobic surfaces.

120# polished surface was smoother(see the SEM image of the surface with 10,000× magnifications) than that coated with SiO_2 nanoparticles. The distribution of nanoparticles outside the scratches was different for the two hydrophobic surfaces. This layer of SiO_2 nanoparticles with micro-scale cavities or islands made the surface with a morphology that tends to increase the number of nucleate sites. The experimental data also proved that at a higher wall superheat, the pool boiling heat transfer was enhanced for the two nanoparticle coated surface. The micro structure of Parylene film coated superhydrophobic surface was different from the two hydrophobic surface. The Parylene particles were randomly deposited onto the micro scratches with typical sizes in the order of 10–50μm. The lump of Parylene film made the surface to be more hydrophobic. Vapor column outside the super hydrophobic surface at higher heat flux deteriorated the pool boiling heat transfer.

The experimental results on hydrophobic surfaces with higher roughness in this paper were also compared with experimental results in the literature, as shown in Figure 13. For the boiling surfaces in literature [37, 38, 48], the variation trends of heat transfer coefficient with heat flux is similar, increasing first and then decreasing. The superheat for critical heat flux of these hydrophobic surfaces are also less, which are about 175kW/m^2, 135kW/m^2, and 55kW/m^2 for literature [37, 38] and [48], respectively. The present experimental result was close in lower heat flux, but greater at higher heat flux, compared to that from literature. For example, the boiling surface roughness (micron scale) of this paper was much larger than that (nano scale) in the literatures. It would be discussed in the following paragraph. Boiling heat transfer performances on superhydrophobic coatings e.g. PTFE fine particles coating reported by Takata [49], Teflon fluoropolymer by Betz [38], Glaco coated by Teodori [34], PTFE by Kim[48] and Parylene film in this paper were shown in Figure 14. It was worth noting that the Glaco coated surface with the greatest hydrophobicity of 166° Contact angle and the smallest roughness of *Ra* = 60nm exhibited the worst heat transfer performance in the four cases, which might be caused by the vapor film around the surface according to

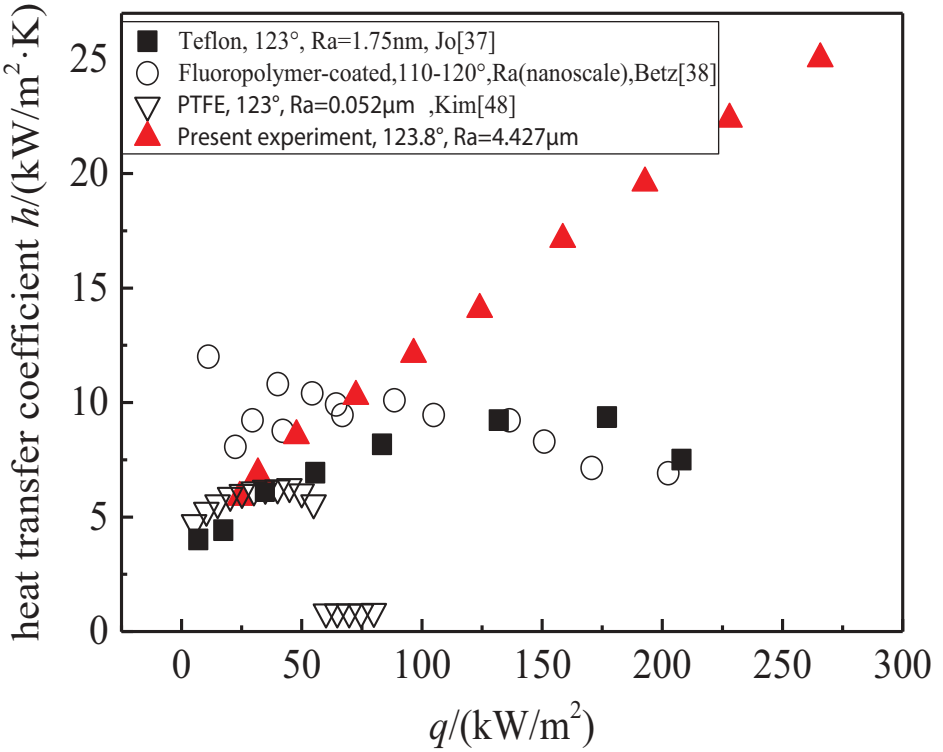

Figure 13. Comparison of present experimental result for the hydrophobic surface with that from literature.

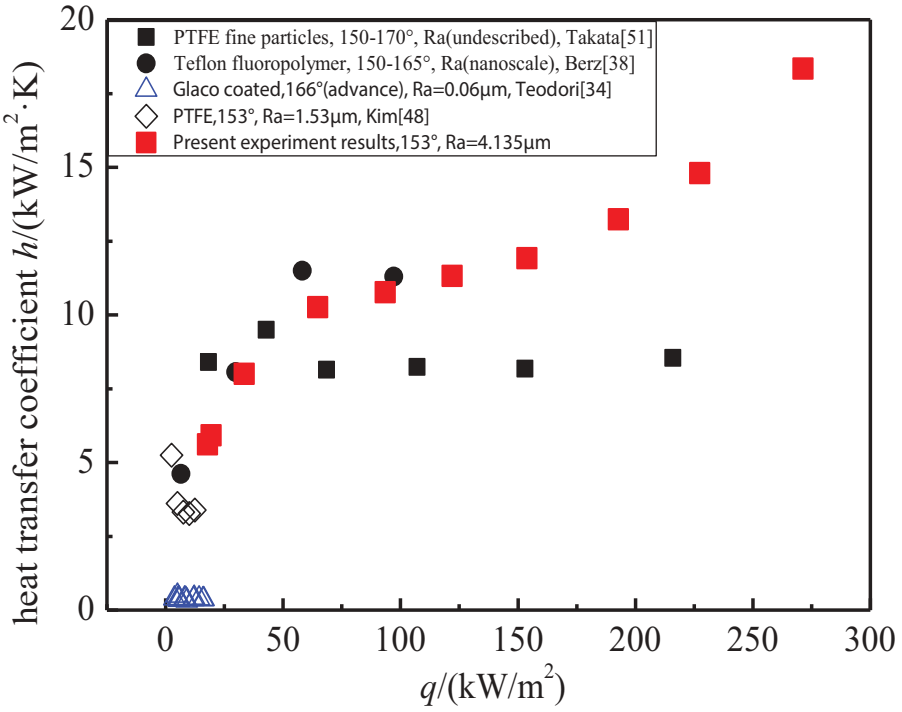

Figure 14. Comparison of present experimental result for the superhydrophobic surface with that from literature.

literature [34]. In addition, the superhydrophobic surfaces in comparsion in Figure 14 also reached the regimes of film boiling at lower superheat. The critical heat fluxes were less than 100kW/m^2. But for hydrophobic surface in the present study, with the largest surface roughness of Ra = 4.135μm, the heat transfer coefficient increased monotonously in the range of the entire boiling regime in study. Until 300kW/m^2, the critical heat flux has not yet been detected. According to the analysis, the nanoparticles coating might loss during the experiment for the hydrophobic surface. The surface might also be a biphilic surface.

Jones et al. [42]. showed that surface roughness can strengthen the pool boiling heat transfer coefficient on the hydrophilic surface because of the intensification of the nucleation sites. Kim et al. [48] also indicated that surface roughness can enhance the critical heat flux with the augmentation of capillary wicking on the hydrophilic surface. How the surface roughness interacts with the wettability outside a hydrophobic surface is still not very clear. Generally, the effect of surface roughness and wettablity on the boiling heat transfer includes three aspects:

(1) Roughness typically has positive effect on the boiling heat transfer for the surface with moderate wettability. It can be explained by the typical bubble nucleation theory in cavities. The present experimental result of deionized water on 360# sand paper roughed surface also proved that. The CHF also increase 10–20% for the sand paper roughed surface[39].
(2) For the super hydrophobic and hydrophobic surfaces with higher roughness, the heat transfer was enhanced in lower superheat and decreased with further increment of superheat. The boiling heat transfer coefficient is less than the smooth surface with moderate wettability at the heat flux of 100kW/m^2 in the present study. This is also supported by the previous studies in [48]. At lower superheat, the flooded effect in reducing the superheat in the cavity is more evident for the surface with higher wettability. That's the reason for the hydrophobic surface can enhance the heat transfer at lower superheat. While, for the

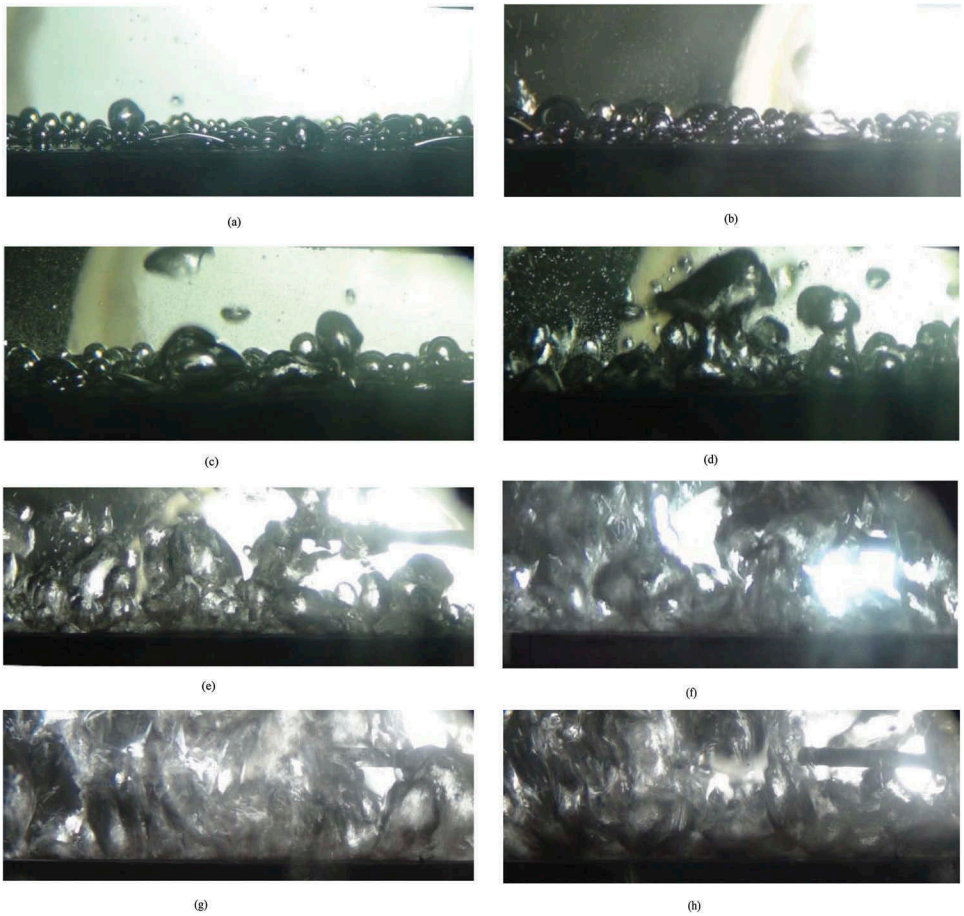

Figure 15. Pool boiling photos of deionized water on the superhydrophobic surface (CA is 153.0°) in different heat flux.

hydrophobic surface, the decreasing rate of heat transfer coefficient seems to be less than that of super hydrophobic surface at higher superheat. As the capillary effect was almost nonexistent for super hydrophobic surface at higher superheat, the value of CHF was lower than hydrophilic surface. At lower superheat, the surface roughness seems to play an important role in the boiling heat transfer. At higher superheat, the wettbility plays a dominant role. It is due to that the surface with any micro-scale roughness was all wrapped by vapor film. Increase of surface roughness on the hydrophobic surface can increase the critical heat flux with the combined effect of capillarity and disturbance on the vapor film. The greater boiling heat transfer coefficient and delayed CHF were all observed in Figure 14 and Ref. [37, 38, 48] for the super hydrophobic surface with higher roughness.

(3) For the hydrophilic or super hydrophilic surface, as the wettability was enhanced, the active nucleation site density decreased and the average heat transfer coefficient also decreased[50]. It is likely that the nucleate cavities can be more easily affected by the flooding due to improved wettibility. While, for the hydrophilic surface with different roughness, it is clear that increase of surface roughness can improve the boiling heat transfer performance over the entire boiling regimes[50]. The roughed surface can certainly provide more nucleate sites for bubble generation. The CHF would also increase with the enhanced wettability. Improved wettability delays the dryout of the heated surface and maintains nucleate boiling at higher superheat [48]. For the hydrophilic surface, increase of roughness can also increase

the CHF. As the increase of surface roughness, capillary effect can be more pervasive for hydrophilic surface. It would lead to an increased CHF [50]. While, the CHF augmentation with increased roughness seems to have its limit [50, 51].

After the investigations, it could be confirmed that the CHF was all augmented with higher roughness for the surface with different wettability. It's difficult to maintain the same wettability with different roughness. The contact angle might also increase as the increase of surface roughness (Table 4). The analysis above is normally based on the general trend. It is the interaction of wettibility and roughness over the entire boiling regime. The effect of roughness includes: providing more cavity, increased surface area and promote the capillary effect.

Boiling visualization analysis and discussion of superhydrophobic surface

In order to further identify the mechanism of boiling heat transfer, the boiling photos on super hydrophobic surface were taken in different heat fluxes as shown in Figure 15. The figures revealed that the vapor bubbles on super hydrophobic surface began to form in very small heat flux. The onset of nucleate boiling (ONB) on the surface occurred earlier than hydrophilic surface. While, the bubble column around the heat transfer surface for the super hydrophobic surface was more considerable compared with hydrophilic surface at higher heat flux. The departing bubbles with much larger radius were also observed on the super hydrophobic surface. Eventually the super hydrophobic surface possessed higher heat transfer coefficient than copper surface in lower heat flux and lower heat transfer coefficient in higher heat flux. The pictures are not clear at higher heat flux. It is due to a large number of bubbles formed and detached rapidly at higher heat flux. The bubble nucleation images can't be clearly shoot even using an advanced high-speed camera.

From Yang and Kim [43], as the increase of contact angle, boiling surface tended to form more number of active cavities and bubble nucleation sites, which would contribute to the enhancement of the heat transfer performance. Super hydrophobic surface had excellent performance in lower heat

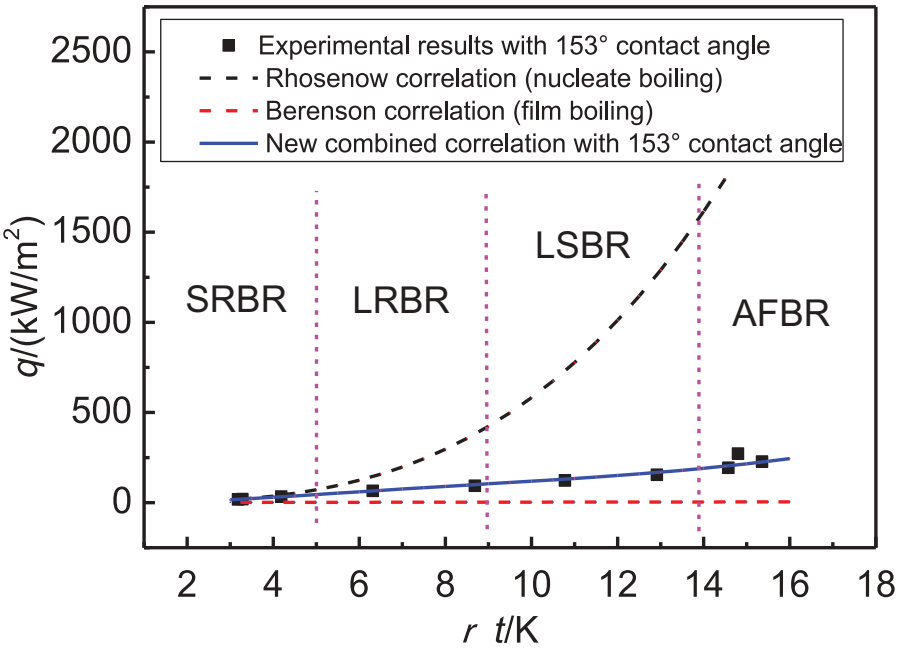

Figure 16. Experimental results for Parylene superhydrophobic film surface compared to the new combined correlation.

flux, thus it would be helpful for heat exchangers in lower heat flux. Nevertheless, with the increase of heat flux beyond a certain limit, the heat transfer degraded. The reason might be that the generated bubbles tended to aggregate or form bigger vapor bubbles more easily in higher heat flux. The properties of aerophily and hydrophobicity of super hydrophobic surface also made it easier to spread aggregated large bubbles on boiling surface to form the local vapor film, which seriously hindered the liquid from flowing to the heating surface as supplement. It increased the thermal resistance and decreased the heat transfer coefficient eventually. However, due to the higher roughness of the surface, the gas-liquid interface in the boiling process was also unstable and changing. The bubbles might be isolated, merged or vapor block interconnected reciprocally outside the super hydrophobic surface.

For pool boiling on hydrophobic surfaces in the experiment, the superficial hydrophobicity benefited to bubble nucleation and increased the nucleation sites number compared with the ordinary copper surface at lower heat flux. For the superhydrophobic surface, at higher heat flux, the increase in the bubble number and the growing in bubble radius, led to aggregation of bubbles and intermittent vapor film. It was detrimental to pool boiling heat transfer. Rohsenow correlation [41] described the law of nuclear boiling heat transfer and had been used in the validation of the boiling apparatus and the experimental procedure. Also, a correlation for film boiling developed by Berenson [52] was also commonly used:

$$q' = C_{wf}\left[\frac{\lambda_v^3\rho_v g(\rho_l-\rho_v)\left(h_{fg}+0.4c_{pv}(T_w-T_s)\right)}{\mu_v(T_w-T_s)\sqrt{\sigma_l/g(\rho_l-\rho_v)}}\right]^{1/4}(T_w-T_s) \tag{7}$$

where q' and C_{wf} represent the heat flux of film boiling heat transfer and the interaction factor between liquid and surface, respectively. For pool boiling heat transfer outside the superhydrophobic surface with higher roughness, the boiling surface was divided into two regions: an isolated bubble region and the steam block region interconnected reciprocally by gas bubbles. So the two correlations (Rohsenow and Berenson correlations) were combined to predict the heat transfer. Two weight coefficients were introduced, and the correlation between the heat flux and wall temperature superheat was given as follows:

$$\begin{aligned} Q &= \omega_n q + \omega_f q' \\ &= \omega_n \mu_l h_{fg}\sqrt{\frac{g(\rho_l-\rho_v)}{\sigma_l}}\left(\frac{c_{pl}}{C_{wl}h_{fg}\,\mathrm{Pr}_l^s}\right)^{\frac{1}{r}}\cdot(T_w-T_s)^{\frac{1}{r}}+ \\ &\quad \omega_f C_{wf}\left[\frac{\lambda_v^3\rho_v g(\rho_l-\rho_v)\left(h_{fg}+0.4c_{pv}(T_w-T_s)\right)}{\mu_v(T_w-T_s)\sqrt{\sigma_l/g(\rho_l-\rho_v)}}\right]^{1/4}(T_w-T_s) \end{aligned} \tag{8}$$

where coefficients ω_n and ω_f represent the areas occupied by the nucleate boiling region and film boiling region in per unit area on the boiling surface, respectively. Their values can also show the contribution of increasing active nucleation sites and bubbles agglomeration into steam film to boiling heat transfer, respectively. Moreover, it is worth noting that the magnitudes of variables ω_n and ω_f are related to the boiling surface superheat, and vary as the experiment proceeds. According to Figure 15, with the increase of heat flux, the number of isolated vapor bubbles decreases almost exponentially and the area occupied by vapor block increases almost exponentially. So ω_n and ω_f are assumed to satisfy the following relations in accordance with exponential law:

$$\omega_n = a_1 + b_1 \cdot c_1^{\Delta t} \tag{9}$$

$$\omega_f = a_2 + b_2 \cdot c_2^{\Delta t} \tag{10}$$

The following relation should be satisfied:

$$\omega_n + \omega_f = 1 \tag{11}$$

ω_n should decrease as the superheat increases, whereas ω_f is opposite. The three coefficients a, b, c are empirical coefficients related to boiling surface material, superhydrophobic film composition, and actual vapor deposition results. And their values a, b, c were obtained by fitting the experimental data.

The experimental result of pool boiling heat transfer for Parylene superhydrophobic film surface with higher roughness was compared with the new combined correlation in Figure 16. From the diagram, the boiling heat transfer law of the superhydrophobic surface of Parylene film was different from that of nucleate boiling (Rhosenow correlation) and film boiling (Berenson correlation). The experimental result was between Rhosenow and Berenson correlations. It was in good agreement with the new combined correlation. This also confirms that the assumptions made in formula (9) and (10) are reasonable.

The pool boiling heat transfer process of the superhydrophobic surface was divided into four stages, as shown in Figures. 16 and 17. The first was the small radius bubble region (SRBR). In this stage, consistent with Figure 15 (a) and (b), the heat transfer was relatively weak, and the radius of bubble was smaller. As the increment of heat flux, the radius of bubble increased and heat transfer was enhanced as shown in Figure 15 (c) and (d). This was called lager radius bubble region (LRBR). The heat transfer of the first two stages at the heat flux lower than about 93kW/m^2 was enhanced compared with pure copper surface due to increased nucleation sites.

As the heat flux continued to increase to higher than 93kW/m^2, also due to the surfacial superhydrophobicity, the vapor bubbles on boiling surface began to reunite with each other to form larger interrupted steam blocks. This region was called large steam block region (LSBR), see Figure 15(e) and (f). As the experiment proceeding, the larger discontinuous steam blocks merged and connected with each other, eventually forming vapor film and diminishing the heat transfer. This was approaching the film boiling region (AFBR) with boiling photos in Figure 15 (g) and (h). It was worth pointing out that the proposed four boiling regions were just qualitative and helpful to understand the superhydrophobic surface boiling process in this article. In fact, there were no obvious dividing lines between the four regions.

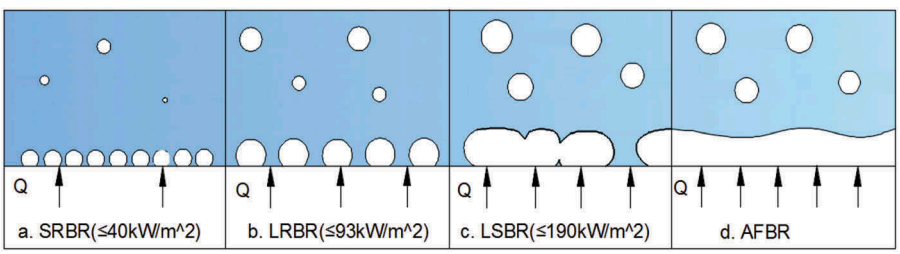

Figure 17. Four stages of pool boiling heat transfer on superhydrophobic surface.

Conclusions

A pool boiling heat transfer test rig was built and pool boiling heat transfer of water and SiO_2 nanofluid on six different surfaces with different wettability and higher roughness was tested at the atmospheric pressure. The heat transfer performances of different boiling surfaces were studied and compared with the pure copper surface. The major findings are as follows:

(1) The hydrophilic silica nanofluid normally had lower heat transfer coefficient compared with deionized water outside different sandpaper roughed surfaces due to the deposition of silica nanoparticles. As the increment of nanofluid mass concentration from 0.025% to 0.1%, a mild reduction of heat transfer coefficient was observed.
(2) The two hydrophobic surfaces behaved similarly in pool boiling heat transfer. The coated nanoparticle might loss during the experiment with the two methods to obtain the hydrophobic surface.
(3) When the heat flux was approximately below 93 kW/m^2, the super hydrophobic surface with higher roughness showed the best heat transfer performance in different surfaces. But when the heat flux passes about 93 kW/m^2, the heat transfer enhancement ratio of super hydrophobic surface was much less as a result of the bubbles merging into large vapor block even local vapor film.
(4) The hydrophobicity of boiling surfaces might decrease the initial surface superheat of nucleate boiling and increase the number of active cavities. While at larger heat flow, boiling heat transfer was weakened due to the formation of vapor blanket.

List of symbols

k	The slope of temperature fitting curve
q	Nucleate boiling transfer heat flux through boiling surface, W/m^2
q'	Film boiling transfer heat flux through boiling surface, W/m^2
Q	Heat flux through superhydrophobic boiling surface, W/m^2
h	Boiling heat transfer coefficients, W·m^{-2}·K^{-1}
c	Boiling HTC enhancement ratio
T_i	Temperature of holes in sample copper block, K
T_w	Boiling surface temperature, K
T_s	Saturated temperature, K
x	Distance between the top row of holes and boiling surface, mm
y	Spacing between adjacent two rows of holes, mm
z	Spacing between adjacent two columns of holes, mm
c_{pl}	Liquid specific heat, J/kg·K
h_{fg}	Latent heat of evaporation, kJ/kg
Pr	Prandtl number
D	Depth of holes, mm
d_p	Diameter of SiO_2 nanoparticles, nm
Ra	Arithmetic average roughness, μm
Rt	Total height of profile, μm
N_a	Number of active cavities per unit surface area, 1/m^2
N_s	Cavity areal density, 1/m^2
R_{max}	Maximum active cavity radii, μm
R_{min}	Minimum active cavity radii, μm
C_{wf}	Empirical coefficient of film boiling
C_{wl}	Empirical coefficient of nucleate boiling

w_n Weight coefficient
w_f Weight coefficient
ONB The onset of nucleate boiling region
R The ratio of surface roughness to film thickness of film boiling
a Correlation coefficient
b Correlation coefficient
c Correlation coefficient

Greek alphabet

λ Thermal conductivity, $W{\cdot}m^{-1}{\cdot}K^{-1}$
μ Dynamic viscosity, $mN{\cdot}s/m^2$
ρ Density, kg/m^3
σ Surface tension, N/m
ϕ Diameter of holes, mm
θ Contact angle, °
β Cavity opening angle, °
Δt Wall superheat, °C
ω Mass concentration of nanoparticles, %
$\phi(R)$ Distribution function for the cavity radius
$\theta(\beta)$ Cavity opening angle distribution function
Δ The vapor film thickness of film boiling, μm

Subscript

i Holes number in sample
a Active cavities
s All cavities
max Maximum value
min Minimum value
s Saturation
w Wall
l Liquid
v Vapor

Funding

This work was supported by the National Natural Science Foundation of China [51776160]; National Key R&D Program of China [2016YFB0601200].

References

[1] S. U. S. Choi and J. A. Eastman, "Enhancing thermal conductivity of fluids with nanoparticles," *ASME-Publications-Fed*, vol. 231, pp. 99–105, 1995.
[2] M. Karimzadehkhouei, M. Shojaeian, K. Şendur, M. P. Mengüç, and A. Koşar, "The effect of nanoparticle type and nanoparticle mass fraction on heat transfer enhancement in pool boiling," *Int. J. Heat. Mass. Transf*, vol. 109, pp. 157–166, 2017.
[3] J. Ham, H. Kim, Y. Shin, and H. Cho, "Experimental investigation of pool boiling characteristics in Al2O3 nanofluid according to surface roughness and concentration," *Int. J. Thermal Sci.*, vol. Vol.114, pp. 86–97, 2017.
[4] X. Quan, D. Wang, and P. Cheng, "An experimental investigation on wettability effects of nanoparticles in pool boiling of a nanofluid," *Int. J. Heat. Mass. Transf*, vol. 108, pp. 32–40, 2017.

[5] I. S. Kiyomura, L. L. Manetti, A. P. Da Cunha, G. Ribatski, and E. M. Cardoso, "An analysis of the effects of nanoparticles deposition on characteristics of the heating surface and on pool boiling of water," *Int. J. Heat. Mass. Transf*, vol. 106, pp. 666–674, 2017.
[6] S. Das, D. S. Kumar, and S. Bhaumik, "Experimental study of nucleate pool boiling heat transfer of water on silicon oxide nanoparticle coated copper heating surface," *Appl. Thermal. Eng.*, vol. 96, pp. 555–567, 2016.
[7] A. Bolukbasi and D. Ciloglu, "Pool boiling heat transfer characteristics of vertical cylinder quenched by Sio2–water nanofluids," *Int. J. Thermal Sci.*, vol. 50, pp. 1013–1021, 2011.
[8] T. Sayahi and M. Bahrami, "Investigation on the effect of type and size of nanoparticles and surfactant on pool boiling heat transfer of nanofluids," *J. Heat. Transfer*, vol. 138, pp. 031502, 2015.
[9] M. M. Sarafraz, T. Kiani, and F. Hormozi, "Critical heat flux and pool boiling heat transfer analysis of synthesized zirconia aqueous nano-fluids," *International. Communications. Heat. Mass. Transfer*, vol. 70, pp. 75–83, 2016.
[10] R. Kathiravan, R. Kumar, A. Gupta, and R. Chandra, "Characterization and pool boiling heat transfer studies of nanofluids," *J. Heat. Transfer*, vol. 131, pp. 081902, 2009.
[11] J. T. Cieslinski and T. Z. Kaczmarczyk, "Pool boiling of water-Al2O3 and water-cu nanofluids on horizontal smooth tubes," *Nanoscale. Res. Lett*, vol. 6, pp. 220, 2011.
[12] A. Amiri, *et al*., "Pool boiling heat transfer of CNT/Water nanofluids," *Appl. Thermal. Eng.*, vol. 71, pp. 450–459, 2014.
[13] R. Kathiravan, R. Kumar, A. Gupta, R. Chandra, and P. K. Jain, "Pool boiling characteristics of multiwalled Carbon Nanotube (CNT) based nanofluids over a flat plate heater," *Int. J. Heat. Mass. Transf*, vol. 54, pp. 1289–1296, 2011.
[14] H. Peng, G. Ding, H. Hu, and W. Jiang, "Influence of carbon nanotubes on nucleate pool boiling heat transfer characteristics of refrigerant–oil mixture," *Int. J. Thermal Sci.*, vol. 49, pp. 2428–2438, 2010.
[15] M. M. Sarafraz and F. Hormozi, "Experimental investigation on the pool boiling heat transfer to aqueous multi-walled carbon nanotube nanofluids on the micro-finned surfaces," *Int. J. Thermal Sci.*, vol. 100, pp. 255–266, 2016.
[16] D. Quéré, "Non-sticking drops," *Rep. Prog. Phys.*, vol. 68, pp. 2495–2532, 2005.
[17] R. Wang, *et al*., "Light-induced amphiphilic surfaces," *Nature*, vol. 388, pp. 431–432, 1997.
[18] H. Yu, *et al*., "Fabrication of durable superamphiphobic aluminum alloy surfaces with anisotropic sliding by HS-WEDM and solution immersion processes," *Surf. Coat. Technol*, vol. 275, pp. 112–119, 2015.
[19] B. J. Zhang, R. Ganguly, K. J. Kim, and C. Y. Lee, "Control of pool boiling heat transfer through photo-induced wettability change of titania nanotube arrayed surface," *International. Communications. Heat. Mass. Transfer*, vol. 81, pp. 124–130, 2017.
[20] C. Kondou, S. Umemoto, S. Koyama, and Y. Mitooka, "Improving the heat dissipation performance of a looped thermosyphon using low-GWP volatile fluids R1234ze(Z) and R1234ze(E) with a super-hydrophilic boiling surface," *Appl. Thermal. Eng.*, vol. 118, pp. 147–158, 2017.
[21] M. Tetreault-Friend, *et al*., "Critical heat flux maxima resulting from the controlled morphology of nanoporous hydrophilic surface layers," *Appl. Phys. Lett*, vol. 108, pp. 243102, 2016.
[22] I. Malavasi, B. Bourdon, P. Di Marco, J. De Coninck, and M. Marengo, "Appearance of a low superheat "quasi-leidenfrost" regime for boiling on superhydrophobic surfaces," *International. Communications. Heat. Mass. Transfer*, vol. 63, pp. 1–7, 2015.
[23] E. Teodori, *et al*., "Effect of extreme wetting scenarios on pool boiling conditions," *Appl. Thermal. Eng.*, vol. 115, pp. 1424–1437, 2017.
[24] F. Villa, A. Georgoulas, M. Marengo, P. D. Marco, and J. D. Coninck, Pool boiling versus surface wettability characteristics, Proceedings of the World Congress on Momentum, Heat and Mass Transfer (MHMT'16), Prague, Czech Republic, April 4-5, pp. 110:1–8, 2016.
[25] L. W. Fan, *et al*., "Subcooled pool film boiling heat transfer from spheres with superhydrophobic surfaces: an experimental study," *J. Heat. Transfer*, vol. 138, pp. 021503, 2015.
[26] Y. Nam, G. Warrier, J. Wu, and Y. S. Ju, Experimental and numerical study of single bubble dynamics on a hydrophobic surface, *ASME 2007 International Mechanical Engineering Congress and Exposition*, Seattle, USA, Nov.11–15, pp. 301–307, 2007.
[27] Y. Li, K. Zhang, M. C. Lu, and C. Duan, "Single bubble dynamics on superheated superhydrophobic surfaces," *Int. J. Heat. Mass. Transf*, vol. 99, pp. 521–531, 2016.
[28] T. J. Hendricks, S. Krishnan, C. Choi, C. Chang, and B. Paul, "Enhancement of pool-boiling heat transfer using nanostructured surfaces on aluminum and copper," *Int. J. Heat. Mass. Transf*, vol. 53, pp. 3357–3365, 2010.
[29] E. Forrest, *et al*., "Augmentation of nucleate boiling heat transfer and critical heat flux using nanoparticle thin-film coatings," *Int. J. Heat. Mass. Transf*, vol. 53, pp. 58–67, 2010.
[30] B. Bourdon, P. D. Marco, R. Rioboo, M. Marengo, and J. D. Coninck, "Enhancing the onset of pool boiling by wettability modification on nanometrically smooth surfaces," *International. Communications. Heat. Mass. Transfer*, vol. 45, pp. 11–15, 2013.

[31] B. Shi, Y. Wang, and K. Chen, "Pool boiling heat transfer enhancement with copper nanowire arrays," *Appl. Thermal. Eng.*, vol. 75, pp. 115–121, 2015.
[32] L. Fan, J. Li, D. Li, L. Zhang, and Z. Yu, "Regulated transient pool boiling of water during quenching on nanostructured surfaces with modified wettability from superhydrophilic to superhydrophobic," *Int. J. Heat. Mass. Transf*, vol. 76, pp. 81–89, 2014.
[33] H. Jo, D. I. Yu, H. Noh, H. S. Park, and M. H. Kim, "Boiling on spatially controlled heterogeneous surfaces: wettability patterns on microstructures," *Appl. Phys. Lett*, vol. 106, pp. 181602, 2015.
[34] E. Teodori, T. Palma, T. Valente, A. S. Moita, and A. L. N. Moreira, Bubble dynamics and heat transfer for pool boiling on hydrophilic, superhydrophobic and biphilic surfaces, *7th European Thermal-Sciences Conference*, Krakow, Poland, June 19–23,, Vol.745, p.032132, 2016.
[35] Z. Zhao, *et al*., "Thermal performance analysis of pool boiling on an enhanced surface modified by the combination of microstructures and wetting properties," *Appl. Thermal. Eng.*, vol. 117, pp. 417–426, 2017.
[36] M. Zupančič, M. Steinbücher, P. Gregorčič, and I. Golobič, "Enhanced pool-boiling heat transfer on laser-made hydrophobic/superhydrophilic polydimethylsiloxane-silica patterned surfaces," *Appl. Thermal. Eng.*, vol. 91, pp. 288–297, 2015.
[37] H. Jo, H. S. Ahn, S. Kang, and M. H. Kim, "A study of nucleate boiling heat transfer on hydrophilic, hydrophobic and heterogeneous wetting surfaces," *Int. J. Heat. Mass. Transf*, vol. 54, pp. 5643–5652, 2011.
[38] A. R. Betz, J. Jenkins, C. C. Kim, and D. Attinger, "Boiling heat transfer on superhydrophilic, superhydrophobic, and superbiphilic surfaces," *Int. J. Heat. Mass. Transf*, vol. 57, pp. 733–741, 2013.
[39] J. Kim, S. Jun, R. Laksnarain, and S. M. You, "Effect of surface roughness on pool boiling heat transfer at a heated surface having moderate wettability," *Int. J. Heat. Mass. Transf*, vol. 101, pp. 992–1002, 2016.
[40] S. J. Kline and F. A. Mcclintock, "Describing uncertainties in single sample experiments," *Mechanical. Eng.*, vol. 75, pp. 3–9, 1953.
[41] S. M. Yang and W. Q. Tao, *Heat Transfer*. Beijing, China: Higher Education Press, 2006, pp. 320–322.
[42] B. J. Jones, J. P. McHale, and S. V. Garimella, "The influence of surface roughness on nucleate pool boiling heat transfer," *J. Heat. Transfer*, vol. 131, pp. 1–14, 2009.
[43] S. R. Yang, R. H. Kim, and A. Mathematical, "Model of the pool boiling nucleation site density in terms of the surface characteristics," *Int. J. Heat. Mass. Transf*, vol. 31, pp. 1127–1135, 1988.
[44] Z. Liu and L. Liao, "Sorption and agglutination phenomenon of nanofluids on a plain heating surface during pool boiling," *Int. J. Heat. Mass. Transf*, vol. 51, pp. 2593–2602, 2008.
[45] D. Milanova and R. Kumar, "Heat transfer behavior of silica nanoparticles in pool boiling experiment," *J. Heat. Transfer*, vol. 130, pp. 185–193, 2006.
[46] C. Gerardi, J. Buongiorno, L. W. Hu, and T. McKrell, "Infrared thermometry study of nanofluid pool boiling phenomena," *Nanoscale. Res. Lett*, vol. 6, pp. 232, 2011.
[47] S. W. Xue, Y. Q. Li, Z. N. Xiao, Y. X. Wang, and K. Li, "Boiling heat transfer characteristics of water-based SiO2 nanofluids," *J. Chem. Ind. Eng.*, vol. (0),, pp. 1–9, 2017.
[48] J. Kim, A. Girard, S. Jun, J. Lee, and S. M. You, "Effect of surface roughness on pool boiling heat transfer of water on hydrophobic surfaces," *Int. J. Heat. Mass. Transf*, vol. 118, pp. 802–811, 2018.
[49] Y. Takata, S. Hidaka, and T. Uraguchi, "Boiling feature on a super water-repellent surface," *Heat. Transfer. Eng*, vol. 27, pp. 25–30, 2006.
[50] J. Kim, S. Jun, J. Lee, J. Godinez, and S. M. You, "Effect of surface roughness on pool boiling heat transfer of water on a superhydrophilic aluminum surface," *J. Heat. Transfer*, vol. 139, pp. 101501, 2017.
[51] A. R. Girard, J. Kim, and S. M. You, Pool boiling heat transfer of water on hydrophilic surfaces with different wettability, in: ASME 2016 International Mechanical Engineering Congress and Exposition, American Society of Mechanical Engineers, 2016, pp. V008T010A018–V008T010A018.
[52] P. Berenson, "Film-boiling heat transfer from a horizontal surface," *J. Heat. Transfer*, vol. 83, pp. 351–356, 1961.